

**CHARACTERISTICS AND RELIABILITY OF CPP-GMR VERSUS TMR  
HEADS: STRIPE HEIGHT AND ASPECT RATIO EFFECTS**



**E076453**

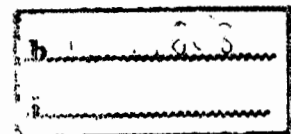


A THESIS SUBMITTED IN PARTIAL FULFILLMENT  
OF THE REQUIREMENT FOR THE DEGREE OF  
MASTER OF ENGINEERING IN DATA STORAGE TECHNOLOGY  
(INTERNATIONAL PROGRAM)  
INTERNATIONAL COLLEGE  
KING MONGKUT'S INSTITUTE OF TECHNOLOGY LADKRABANG

2012

KMITL-2012-IC-M-005-002

เลขหมู่.....  
เลขทะเบียน..... **76453**  
วัน,เดือน,ปี..... **25** ส.ค. 2557





**COPYRIGHT 2012**

**INTERNATIONAL COLLEGE**

**KING MONGKUT'S INSTITUTE OF TECHNOLOGY LADKRABANG**

This material is reserved for educational use only, not allowed for commercial use.

Forbidden to modify the content, and cite the document when use.

|                       |   |
|-----------------------|---|
| <b>Thesis Title</b>   | Characteristics and Reliability of CPP-GMR versus TMR heads: Stripe Height and Aspect ratio effects       |
| <b>Student</b>        | Miss Saowarat Kamwan  |
| <b>Student ID</b>     | 52600620  |
| <b>Degree</b>         | Master of Engineering   |
| <b>Program</b>        | Data Storage Technology (International Program)   |
| <b>Year</b>           | 2012  |
| <b>Thesis Advisor</b> | Dr. Winadda Wongwiriyanan<br>Assoc. Prof. Dr. Wanchai Pijitrojana<br>Asst. Prof. Dr. Chiranut Sa-ngiamsak |

## ABSTRACT

The hard disk drive industry has been facing strong competition from other data storage devices. The primary reader technology is based on the Giant magnetoresistance (GMR) and Tunneling magnetoresistance (TMR). The TMR head will likely reach its limit at the  $2\text{Tbit/in}^2$  recording density because of its high impedance effect on the bit rate of the signal. To overcome this limit, CPP-GMR reader using all metallic materials and current perpendicular to plane (CPP) geometry has to be employed for areal density  $>2\text{Tbit/in}^2$ . In this study we focused on physical dimension designs of a CPP-GMR head. We performed experiment, CPP-GMR and TMR sensors were fabricated to achieve same aspect ratio (AR). AR is stripe height (SH) divided by track width (TW). The characteristics and reliability were study by quasi static test (QST). Selected a CPP-GMR using a Cu spacer shows an opportunity to scale down the reader dimensions (SH and TW) while TMR sensor shows very high resistance because of its MgO insulator barrier. CPP-GMR has the advantage of low RA but has a drawback in terms of low signal to noise ratio (SNR). CPP-GMR sensor shows MR resistance 7 times and amplitude 24 times less than TMR sensor at AR 1.0 at the same quasi static test (QST) condition; 140mV bias, measurement magnetic field: 520Oe and sweep field:  $\pm 520\text{Oe}$ . In terms of stability and noise, barkhausen jump,

This material is reserved for educational use only, not allowed for commercial use.

hysteresis and static SNR, the CPP-GMR sensors show worse than TMR at all AR ranges. This is because the amplitude measurement of CPP-GMR may not be suitable as we measured at the same condition as TMR. There are 2 reliability evaluations in this study, high temperature stress and break down voltage (BDV). At the highest temperature, 120 degree Celsius, CPP-GMR shows a resistance drop of 10% and amplitude drop of 30% compared to TMR shows more than a 30% resistance drop and 8% amplitude drop. The resistance and amplitude return back to normal when the temperature cools down for both CPP-GMR and TMR sensors. CPP-GMR and TMR sensors show different phenomena at high voltage bias. The resistance of CPP-GMR increases more than 30% at bias voltage 420 mV while TMR decreases more than 30% at bias voltage 600mV. Although 2 types of magnetic read sensors (CPP-GMR & TMR) show different damage symptom the results are the same, the magnetic read sensor cannot work anymore. CPP-GMR shows an opportunity to scale down without a large resistance increase. From this study, suggestions can be made to manufacturing since available CPP-GMR sensors had unexpected characteristics and reliability when compared to TMR sensors. Further additional improvements in magnetic read sensors such as magnetic material, spacer, optimized RA and other layers of sensors need to be considered. In terms of time and cost savings, we can suggest the WD production team to minimize the AR range, reduce sample size and groups to achieve suitable AR. We cannot follow standard AR =1 because the wafer fabrication process cannot control process well enough. In terms of process improvements, we should check WDB slider fabricated lapping process and consider a resistance specification limit to get high quality TMR. (Refer to BDV result)

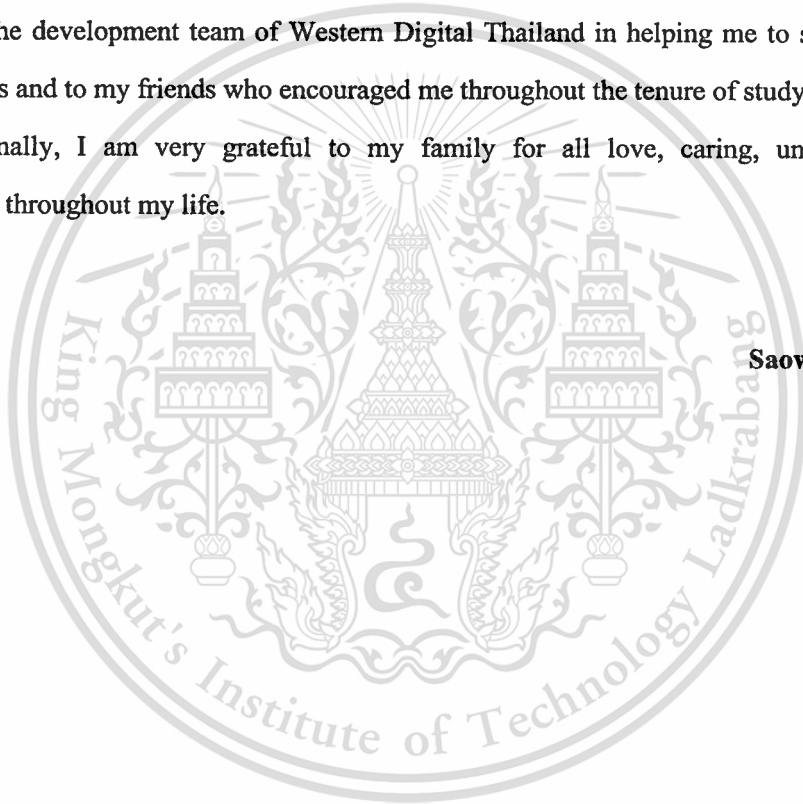
## ACKNOWLEDGEMENT

I would like to extend my sincere gratitude to my advisor Assoc. Prof. Dr. Wanchai Pijitrojana, Asst. Prof. Dr. Chiranut Sa-ngiamsak and Dr. Winadda Wongwiriyan in advising me for this research work. I would like to appreciate the thesis committees for their precious time and advices to give an admirable shape to this thesis.

I really appreciate to Western Digital Company which provided the full scholarship for studying in the master program, experiment materials and equipments. At the same time, I would like to thank all my colleagues who supported to identify the tools and the samples for my research, the development team of Western Digital Thailand in helping me to setup and testing the samples and to my friends who encouraged me throughout the tenure of study and research.

Finally, I am very grateful to my family for all love, caring, understanding and motivation throughout my life.

**Saowarat Kamwan**

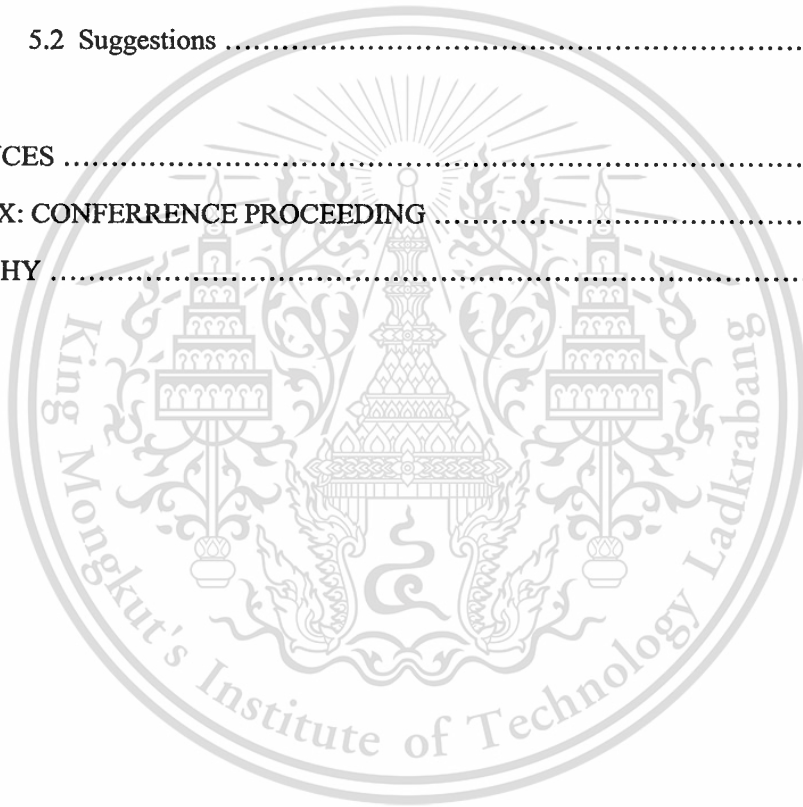


# CONTENTS

|  | Page |
|--|------|
| ABSTRACT .....   | I    |
| ACKNOWLEDGEMENTS .....   | III  |
| CONTENTS .....   | IV   |
| LIST OF TABLES .....   | VI   |
| LIST OF FIGURES .....  | VII  |
| <br>   |      |
| CHAPTER 1 INTRODUCTION .....   | 1    |
| 1.1 Significance and Background .....                                    | 1    |
| 1.2 Objectives .....   | 5    |
| 1.3 Scopes .....   | 5    |
| 1.4 Limitations .....  | 6    |
| 1.5 Expected Benefits .....  | 6    |
| <br>   |      |
| CHAPTER 2 LITERATURE REVIEW .....  | 7    |
| 2.1 Areal density tendency .....   | 7    |
| 2.2 CPP-GMR previous study .....   | 12   |
| 2.3 CPP-GMR technology opportunity .....                                 | 17   |
| 2.4 Principle and Theory of Magnetic Read Sensor .....                   | 20   |
| 2.5 Characteristics and Reliability study for Magnetic Read Sensor ..... | 27   |
| 2.6 Conclusion .....   | 32   |
| <br>   |      |
| CHAPTER 3 RESEARCH METHODOLOGY .....                                     | 34   |
| 3.1 Slider Fabrication Process .....                                     | 34   |
| 3.2 Experiment Details.....  | 37   |
| 3.3 Characteristics of Magnetic Read Sensors .....                       | 38   |
| 3.4 Reliability test conditions.....                                     | 41   |
| 3.5 List of Materials and Research tools.....                            | 42   |

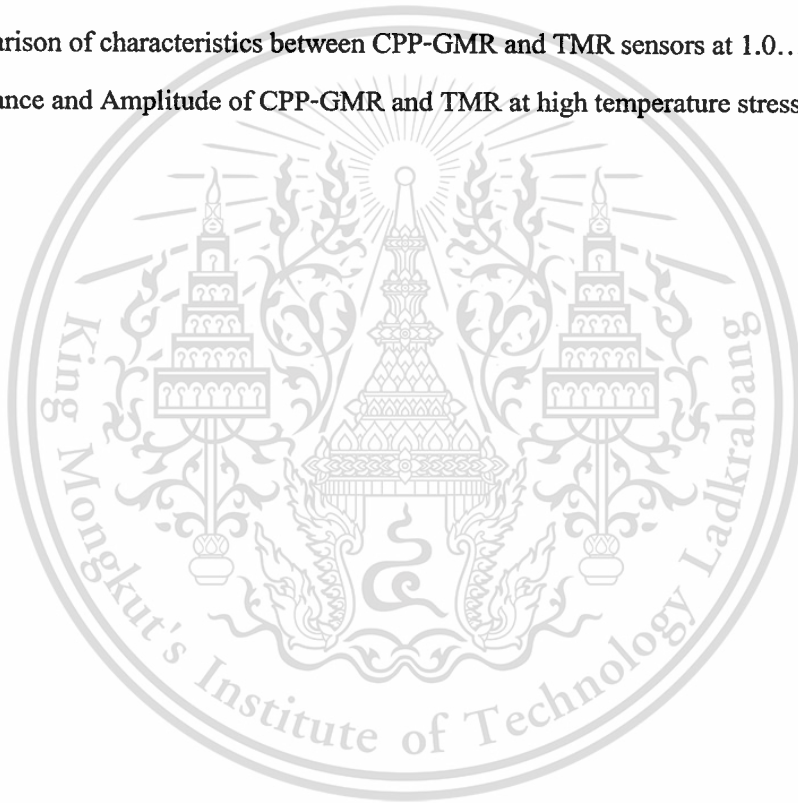
## CONTENTS (CONT.)

|   | Page |
|---|------|
| CHAPTER 4 RESULTS AND ANALYSIS OF DATA .....            | 43   |
| 4.1 Characteristics of CPP-GMR versus TMR sensors ..... | 43   |
| 4.2 Reliability of CPP-GMR versus TMR sensors .....     | 48   |
| 4.3 Conclusion .....                                    | 51   |
| CHAPTER 5 CONCLUSIONS AND SUGGESTIONS .....             | 53   |
| 5.1 Conclusions and discussions .....                   | 53   |
| 5.2 Suggestions .....                                   | 54   |
| REFRENCES .....   | 55   |
| APPENDIX: CONFERENCE PROCEEDING .....                   | 57   |
| BIOGRAPHY .....   | 62   |



## LIST OF TABLES

| Table   | Page |
|---|------|
| 2.1 Simulation condition.....   | 14   |
| 2.2 Representative dimensions of the recording system for a HDD product<br>with areal density of 80Gbit/in <sup>2</sup> ..... | 21   |
| 2.3 Critical thickness and Lateral, Read width Requirements in Year2010.....  | 27   |
| 3.1 Stripe height (SH) and Aspect ratio (AR) for CPP-GMR & TMR .....  | 37   |
| 3.2 High temperature stress conditions .....  | 41   |
| 4.1 Comparison of characteristics between CPP-GMR and TMR sensors at 1.0.....   | 44   |
| 4.2 Resistance and Amplitude of CPP-GMR and TMR at high temperature stress .....  | 50   |



## LIST OF FIGURES

| Figure   | Page |
|--|------|
| 1.1 SCR Road map of May 2009.....  | 2    |
| 1.2 Close-up view of recorded bits with a recorded track .....   | 3    |
| 1.3 Recording head dimensions compared to track dimensions on the disk .....   | 4    |
| 2.1 Bit length as a function of areal density at various fixed BARs .....  | 8    |
| 2.2 Track width as a function of areal density at various fixed BARs .....   | 8    |
| 2.3 Comparative study of DDSV and ADSV .....   | 9    |
| 2.4 Future Technology Options for HDD Storage .....  | 10   |
| 2.5 Areal density R&D Targets .....  | 11   |
| 2.6 Pros and Cons of Technology Options .....  | 11   |
| 2.7 Projected reader noise for a range of recording density .....  | 13   |
| 2.8 MR ratio dependence on RA .....  | 15   |
| 2.9 Cross sectional HRTEM of CPP-GMR film .....  | 16   |
| 2.10 Calculated SNR versus sensor width for three kinds of reader .....  | 17   |
| 2.11 Trends of data transfer rate for high-eng HDD systems and allowed RA with<br>CPP structure versus areal density ..... | 19   |
| 2.12 CPP-GMR structure used for calculating $\Delta$ RA .....  | 20   |
| 2.13 Thin-film head structure as viewed from the media disk surface .....  | 22   |
| 2.14 Disk-view schematic of CIP GMR sensor .....   | 22   |
| 2.15 Signal transition fields from the recorded media for TMR or CPP-GMR .....   | 23   |
| 2.16 $\Delta$ R/R (%) vs RA for CPP-GMR and TMR .....  | 24   |
| 2.17 Read width definition using CMP-based liftoff process .....   | 25   |
| 2.18 ABS TEM cross section of a 90 nm wide CIP GMR read sensor .....   | 26   |
| 2.19 ABS TEM cross section of a 95 nm TMR read sensor .....  | 26   |
| 2.20 High frequency noise spikes could be induced as well as be cured by cumulative<br>ESD pulses for MTJ readers .....    | 28   |
| 2.21 Variations in TMR curves with temperature a) DB MTJ and b) SB MTJ .....   | 29   |
| 2.22 Temperature dependence of a) the coercive field for each layer and<br>b) TMR curves for DB MTJ and SB MTJ .....       | 30   |

## LIST OF FIGURES (CONT.)

| Figure  | Page |
|---|------|
| 2.23 Bias voltage dependence of TMR for DB MTJ and SB MTJ .....                           | 30   |
| 2.24 Schematic illustration of electron tunneling in ferromagnet/insulator/ferromagnet... | 32   |
| 3.1 Slider fabrication process flow .....   | 35   |
| 3.2 Slider component.....   | 36   |
| 3.3 Slider ABS side.....  | 36   |
| 3.4 Quasi Static Tester (QST).....  | 38   |
| 3.5 Transfer curve (TC) of Magnetic recording sensor.....                                 | 39   |
| 3.6 Barkhausen Jump Phenomena of Magnetic Read Sensor.....                                | 40   |
| 3.7 Hysteresis Phenomena of Magnetic Read Sensor.....                                     | 40   |
| 4.1 Resistance of CPP-GMR and TMR with different AR.....                                  | 44   |
| 4.2 Amplitude of CPP-GMR and TMR with different AR.....                                   | 45   |
| 4.3 Zoom-In Amplitude of CPP-GMR with different AR.....                                   | 45   |
| 4.4 Percent Resistance change at different AR compared to AR1.0 .....                     | 46   |
| 4.5 Percent Amplitude change at different AR compared to AR1.0 .....                      | 46   |
| 4.6 Static SNR of CPP-GMR and TMR with different AR .....                                 | 47   |
| 4.7 Barkhausen Jump (%) of CPP-GMR versus TMR with different AR .....                     | 48   |
| 4.8 Hysteresis (%) of CPP-GMR versus TMR with different AR .....                          | 48   |
| 4.9 Percent Resistance change at high temperature stress .....                            | 49   |
| 4.10 Percent Amplitude change at high temperature stress .....                            | 50   |
| 4.11 Break down voltage test result of CPP-GMR sensors .....                              | 51   |
| 4.12 Break down voltage test results of TMR sensors .....                                 | 51   |

# CHAPTER 1

## INTRODUCTION

### 1.1 Significance and Background

The hard disk drive industry has been facing strong competition from other data storage devices such as solid state drive. In order to sustain market share in cost and capacity, the areal density should be maintained growth rate of 30% to 40% per year therefore hard disk drive technology with areal density of 10 Tbit/in<sup>2</sup> should be developed around year 2015 [1] & [2].

Areal density growth of research targets versus recent studies and actual manufacturing in HDD factory shown in figure 1.1. The hard disk drive industry is expected to demonstrate and manufacture the 2Tbit/in<sup>2</sup> technology and products in the years 2012 and 2015, respectively. Actually in the factory we can produce only about 700-800Gbit/in<sup>2</sup> recording density, that means we have some opportunity to develop more to achieve higher recording density. Tunneling magnetoresistance (TMR) reader will likely reach its limit at the 2Tbit/in<sup>2</sup> recording density because of its high impedance effect on the bit rate of the signal. To overcome this limit, CPP-GMR reader using all metallic materials and current perpendicular to plane (CPP) geometry has to be employed for areal density >2Tbit/in<sup>2</sup> [3].

Nowadays the areal density annual growth is exposed by many problems such as higher tracks per inch (TPI), writer ability, signal to noise ratio (SNR), adjacent track interference (ATI), wide area erasure, media thermal stability, bit error rate (BER) and high data rate switching issues. To solve these difficulties, a number of competing technologies have been discussed in many previous researches [4]. The most important components in hard disk drive system are media, magnetic writer transducer and magnetic read sensor. We cannot study all of them same time so only magnetic read sensor will be focused in this study.

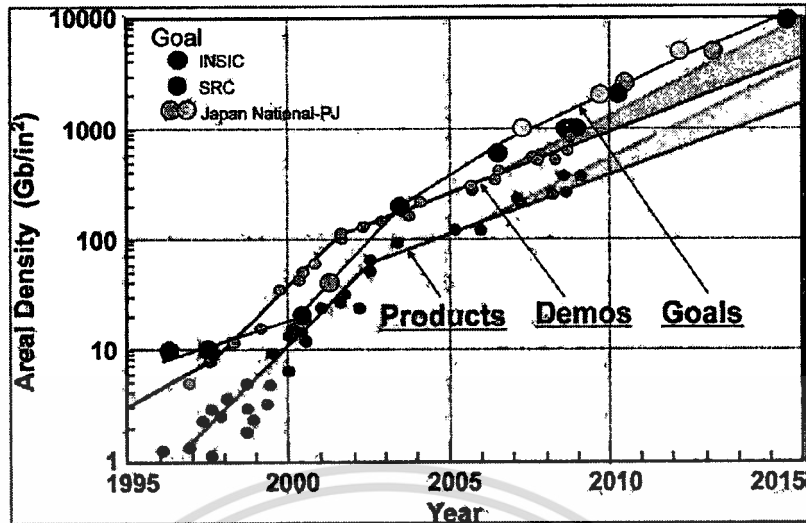
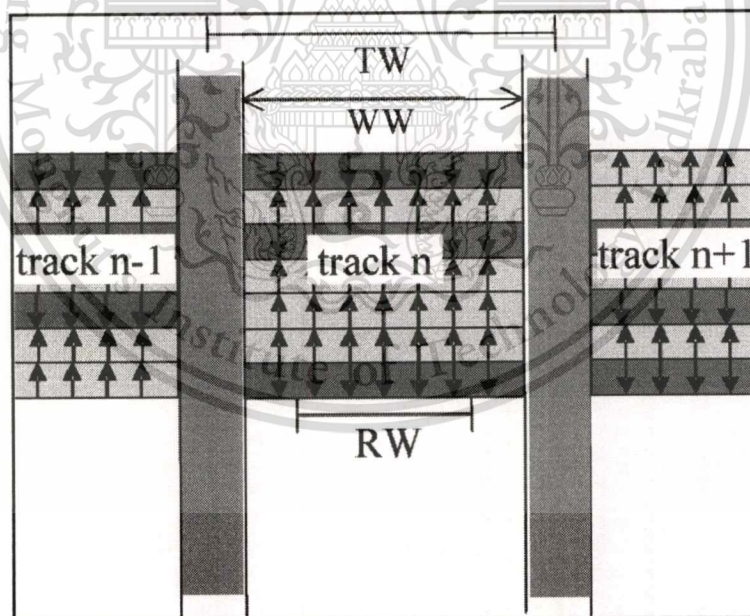


Figure 1.1 SCR Road map of May 2009. [3]

The primary reader technology based on the giant magnetoresistance (GMR) and tunneling magnetoresistance (TMR). The interplay between current head technology giant magnetoresistance with current in plane (CIP-GMR) then moved to tunneling magnetoresistance with current perpendicular to plane (CPP-TMR) and the potential alternative for next generation is giant magnetoresistance with current perpendicular to plane geometry (CPP-GMR). Thus we planned to study the characteristics, reliability and potential advantages of next-generation magnetic read head especially CPP-GMR sensors in perpendicular recording system.

Magnetic reading head (MRH) technology is to optimize the geometrical and environmental constraints under read operations. The recording head can be thought of having three main components: (1) the magnetic reading head sensor, which is the subject of this study; (2) magnetic recording head or write transducer head, which is a micro-fabricated planar electromagnet with a narrow pole that creates a high density of magnetic flux in closeness to the media; and (3) the slider, which is a shaped piece of substrate (usually alumina titanium carbide) onto which the magnetic read sensor and writer transducer head are located, and is engineered to 'fly' only a few nanometers above the extremely spinning magnetic disk.

Figure 1.2 shows the bit geometry within a track is determined by the geometry of the magnetic read sensor, areal density for a particular recording system is the product of the tracks per inch (TPI) in the cross-track direction and the bits per inch (BPI) within a track. A write pole width (WW), a sensor width or read width (RW), and a sensor gap separation between shields or total gap (TG) are shown in Figure 1.3. The width of the written bit is approximately equal to WW (but slightly larger due to fringing effects of the writing fields), and Figure 1.2 shows the final bit geometry on the disk surface. The guard band width, or empty space between written tracks, is typically set at 20% of WW to isolate the bits from adjacent track transition interference. The sensor width RW is only about 60% of WW to allow for tolerance in the placement of the sensor over the written transition during the read or detection operation. Along the track direction, isolation of the sensor from fields emanating from transitions extraneous to the one being sensed is provided by two magnetic shields placed above and below the sensor with a total separation gap (TG).



**Figure 1.2** close-up views of recorded bits with a recorded track. [5]

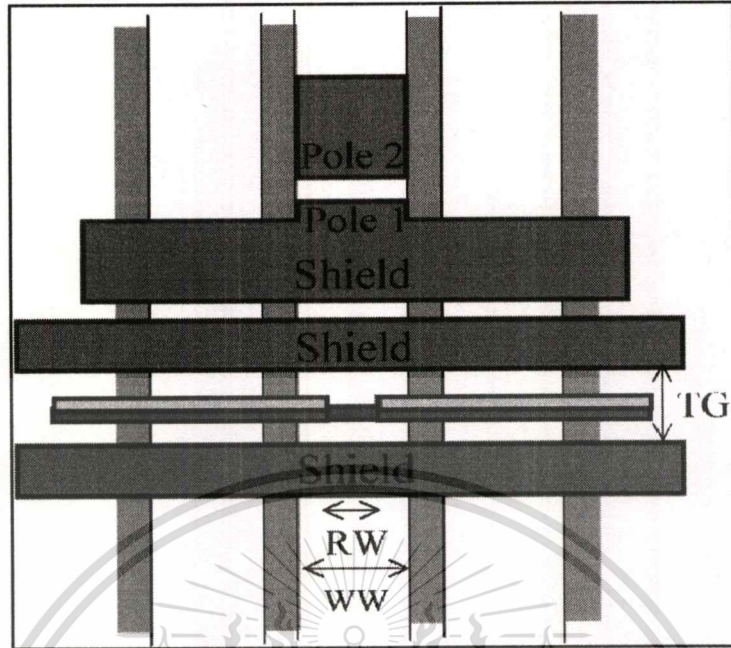


**Figure 1.3** Recording head dimensions compared to track dimensions on the disk. [5]

Figure 1.2 and 1.3 show the critical dimensions of magnetic recording system. As we know, areal density increasing will drive all dimensions to be decrease as much as possible. Then we planned to study the characteristics, reliability and potential advantages of next generation magnetic read head especially CPP-GMR sensors with different aspect ratio (track width and stripe height ratio). The varying aspect ratio (AR) will suggest us how small we can achieve using current TMR and available CPP-GMR sensors.

## 1.2 Objectives

In this experiment the early designed Giant magnetoresistance with current-perpendicular-to-plane (CPP-GMR) from WD design team and current technology tunneling magnetoresistance (TMR) from WD manufacturer were used. The objectives of this research are

1.2.1 To study characteristics and reliability of the CPP-GMR and TMR sensors which is vary stripe height (SH) and aspect ratio (AR) using quasi static tester (QST).

1.2.2 To study reliability, high temperature stress and break down voltage (BDV), CPP-GMR and TMR at same AR 1.0

1.2.3 To design physical dimensions (TW and SH) of CPP-GMR to achieve higher recording density.

## 1.3 Scopes

We focused on the characteristics and reliability of various aspect ratios (varying from 0.4 to 1.6) samples for both CPP-GMR and TMR sensors on key performances such as magnetic resistance, sensitivity or amplitude and static SNR.

1.3.1 This study will be focus on CPP-GMR sensor which is different physical design, various aspect ratios (AR) from 0.4 to 1.6.

1.3.2 The performance of CPP-GMR sensor in this study using quasi static tester (QST). This will provide rapid and effective feedback results to design team.

## 1.4 Limitations

1.4.1 In this study we used CPP-GMR sensor which are fabricated in WD US factory, they are not feasible to change the magnetic material and other designs except physical dimension which can be provided in WD Bang pa-in plant. Thus we vary only aspect ratio (AR)

1.4.2 CPP-GMR, different aspect ratios, was characterized by quasi static testers (QST), which are not the finish values of the HDD system. Final results of HDD performances are required to find the combination between the magnetic read sensors and the read channel. This study is only initial characterization of magnetic read sensor.

1.4.3 This study was based on current available perpendicular recording system (PMR).

1.4.4 The sample sizes selected are limited to 500 to 1000 samples due to specific range of aspect ratios 0.4 to 1.6 each AR has quantity about 500 to 1000 heads.

## 1.5 Expected Benefits

1.5.1 Understanding the characteristics and reliability new candidate magnetic read sensor CPP-GMR and conventional TMR.

1.5.2 Capability in developing and improving slider fabrication process (the hard disk drive manufacturing in Thailand) to support new magnetic read sensor technology.

## CHAPTER 2

### LITERATURE REVIEW

The related theory and literature review of thesis topic of Characteristic and Reliability of CPP-GMR Vs TMR total fifteen papers reviewed for this study to understand the topic. The papers are organized and separated by groups as follow.

- 1) Areal density trend of HDD technology [1] and [2]
- 2) CPP-GMR previous study [3], [4], [7] and [8]
- 3) CPP-GMR technology opportunity [9] and [10]
- 4) Principle and Theory of Magnetic Read Sensor [5], [6] and [13]
- 5) Characteristic and Reliability study of Magnetic Read Sensor [11], [12], [14] and [15]

#### 2.1 Areal density tendency

There are HDD technology have many candidate to cross limitation of higher areal density for example bit patterned magnetic recording (BPMR), heat assisted magnetic recording (HAMR), and microwave assisted magnetic recording (MAMR).

In [1] Perspectives of Read Head Technology for 10Tbit/in<sup>2</sup> Recording, They review magnetic read sensor design, two of the most important parameters are the resolution and the signal to the noise ratio (SNR). For 10Tbit/in<sup>2</sup> recording, the sensor dimensions required to achieve the resolutions are resulting for various bit aspect ratio (BAR) designs. It is shown that the today's shielded read head technology is unable to scale down to meet the linear density requirement. By analyzing the data rate necessities at various BAR values as shown in Figure 2.1 and Figure 2.2

Bit aspect ratio (BAR) is referred to sensor dimensions, defined by below equation.

$$\text{Areal density} = \text{Track density (TD)} \times \text{Bit density (BD)} \quad (2.1)$$

$$\text{Areal density} = \text{BD}^2 / \text{BAR} = \text{TD}^2 \times \text{BAR} \quad (2.2)$$

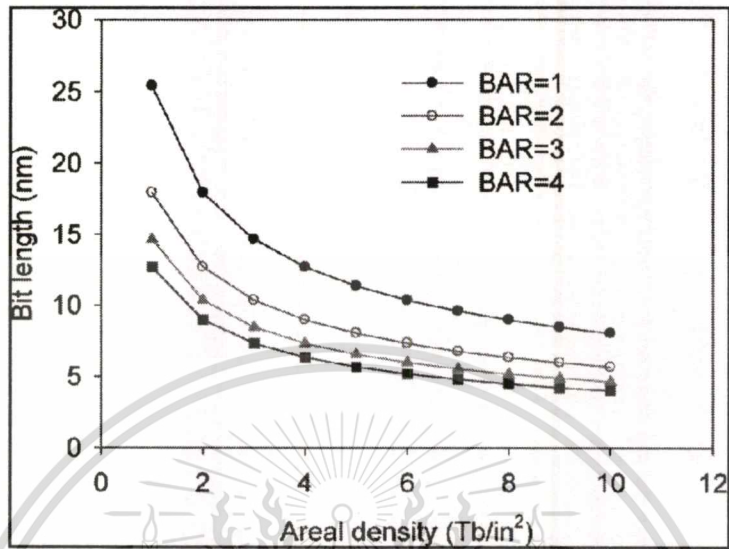


Figure 2.1 Bit length as a function of areal density at various fixed BARs. [1]

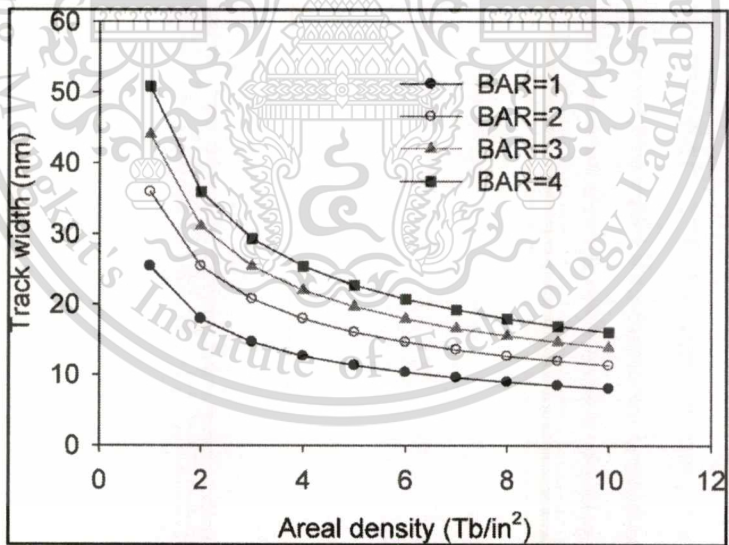
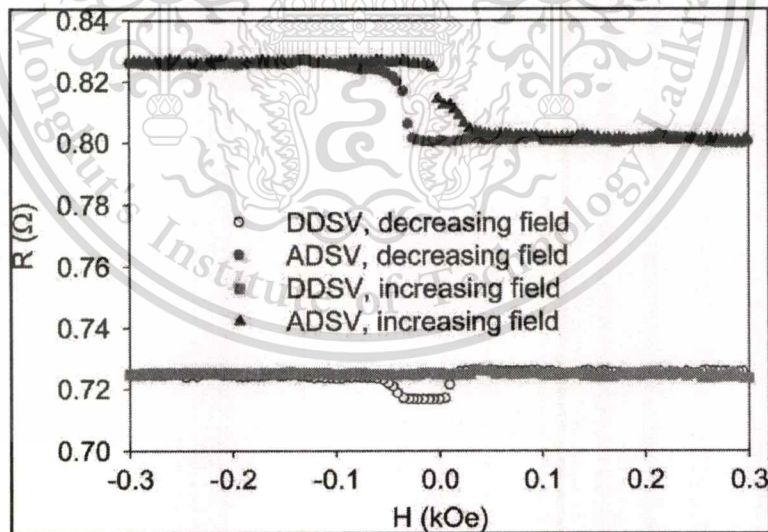


Figure 2.2 Track widths as a function of areal density at various fixed BARs. [1]

It is argued that the current tunneling magnetoresistance (TMR) sensor is no longer suitable to provide high SNR due to its high impedance. A differential dual spin valve (DDSV), which does

not need to have magnetic shields, is proposed to achieve the required SNR and linear resolution of the read head for  $10\text{Tbit/in}^2$ . A systematical investigation on the effect of stiffness field, magnetic shields and media field shows that thermally activated magnetic noise may not necessarily be a crucial limiting factor for  $10\text{Tbit/in}^2$ . The predictable path to increase SNR by increasing GMR ratio is still applicable. Assuming practical constraints and requirements, they come out with the DDSV sensor specifications for  $10\text{Tbit/in}^2$  recording with a stiffness field of  $300\text{Oe}$  and an operating current density of  $4 \times 10^7\text{A/cm}^2$ , a SNR of 20 dB can be achieved under a media field of  $300\text{Oe}$  for an unshielded DDSV sensor having a GMR ratio of 12%. Preliminary studies show that DDSV sensor is very promising for the application in  $10\text{Tbit/in}^2$ . The differential effect in DDSV sensor is established using two types of dual spin valve have shown in Figure 2.3. For a dual spin valve with two reference layer (RL) magnetizations in the same direction, the total resistance change under uniform field is the sum of two spin valves as expected, while for another similar dual spin valve with the two RL magnetizations in the opposite direction, no resistance change is observed in the dynamic field region  $\pm 300\text{Oe}$ .



**Figure 2.3** comparative studies of DDSV and ADSV. [1]

In [2] Future Options for HDD Storage, The HDD industry is at a serious technology cross roads and it is dominant that we quickly establish inclusive paths to push further than the superparamagnetic limit. Figure 2.4 shows several talented technology options have been explored to increase the areal density beyond the limit such as bit patterned magnetic recording (BPMP), heat assisted magnetic recording (HAMR), and microwave assisted magnetic recording (MAMR).

Besides these three technologies, there is recent interest in a fourth approach that has the advantage of staying with a relatively conservative perpendicular medium and head. This combines shingled write recording (SWR) and 2-D read back and signal processing. Either technique can be used separately to give large gains and the combination of the two, which is referred to as 2-D magnetic recording (TDMR), promises particularly large gains. Recording with energy assist on BPM or 2-D signal processing will enable the areal density beyond around  $5\text{Tbit/in}^2$ , even though none of them have shown a clear solution. Previous competitive researches have recently started targeting  $2\text{Tbit/in}^2$  by 2010 for SRC,  $5\text{Tbit/in}^2$  by 2013 for NEDO and  $10\text{Tbit/in}^2$  by 2015 for INSIC. This paper reviews the technology options ahead and the pros & cons for each option.

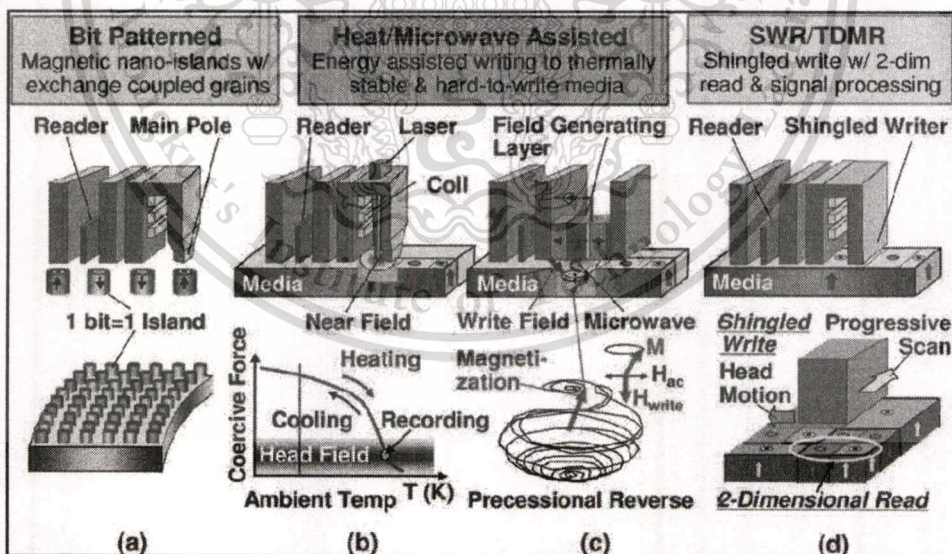


Figure 2.4 Future Technology Options for HDD Storage. [2]

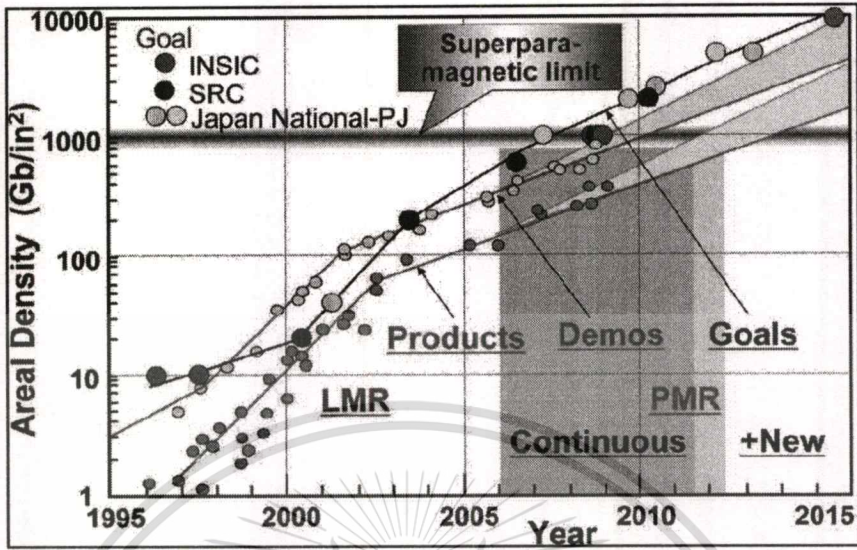


Figure 2.5 Areal density R&D Targets. [2]

|                     |                  | Most Challenging       | Challenging                     | Pros                 |                         |
|---------------------|------------------|------------------------|---------------------------------|----------------------|-------------------------|
|                     |                  | BPMR                   | HAMR                            | MAMR                 | SWR/TDMR                |
| Head                | $T_{wv}$ (MP)    | Small                  |                                 | Large                |                         |
|                     | Assist           | -                      | Near Field                      | Microwave            | -                       |
| Media               | Writability      | Easy-to-write          |                                 | Hard-to-write        |                         |
|                     | Magnetic Feature | Exchange Coupled       | Low $T_c$ Rapid Cool            | Low Damping Constant | Conventional Granular   |
| Servo/ Mecha        | TMR              | Larger                 |                                 | Extension            | Larger (TDMR)           |
|                     | Adaptive         | Difficult              |                                 | Extension            |                         |
| Spacing (Challenge) |                  | Planarization          | Protrusion                      |                      | Extension               |
| R/W                 | High BPI         | Lithography            |                                 | Dual Gradient        | Extension               |
|                     | High TPI         | Lithography            | Thermal Disty?                  | FGL Width            | Fringe Grad             |
|                     | $\Delta E/ATE$   | Small                  | Large?                          |                      | Small                   |
|                     | Data Rate        | Low if BAR is not high | Limit by heat-up and down       |                      | Extension               |
| Signal Processing   |                  |                        | One dimensional                 |                      | Two Dimensional         |
| Architecture        |                  | Synchronous Writing    | Assist Methodology Optimization |                      | New Format Architecture |
| Challenge           | Technology       | Synchronous Writing    | High Temp Reliability           | Microwave Oscillator | New Format Architecture |
|                     | Cost             | Lithography            | Optics                          | -                    | Extra Memory            |

Figure 2.6 Pros and Cons of Technology Options [2]

Figure 2.6 shows none of those options show a clear problem-free solution at this moment. Substantial, carefully-coordinated precompetitive research will strongly be optimistic to fully assess the viability of those options. Thus development activities never stop in hard disk drive technology.

## 2.2 CPP-GMR previous study

There are 6 papers are reviewed in this group, previous study for CPP-GMR sensor show that 2-5 Tbit/in<sup>2</sup> areal density required higher resistance area RA about 0.1-0.3Ω.μm<sup>2</sup> for more stable spin transfer torque (STT). Magnetic read sensor dimensions track width, stripe height and read gap need to be decreased as follow the simulation result in table 2.1. As we know that GMR using metallic spacer which is different from TMR using insulator, many previous studies focused on spacer for instant CPP-GMR sensor with ZnO crystalline barrier is very attractive candidate of future magnetic read sensor in HDDs because very promising trend in term of Johnson noise fitted at 400 K. This confirmed that we need to consider all magnetic material and the quality of barrier for CPP-GMR sensor. However signal to noise ratio (SNR) is very important parameters for magnetic reader sensor either TMR or CPP-GMR.

Recently developed CPP-GMR sensor showed the MR ratio of 18%-19% with the RA product of 0.2-0.3 Ω.μm<sup>2</sup> and achieved 30 dB or more in SNR when track width was 40 nm or larger and showed potential for an areal density of ≥500Gbit/in<sup>2</sup>. CPP-GMR still has some points to be improved; however it is believed that the CPP-GMR will actualize a next high-performance magnetic read sensor in no distant future.

First paper is about 2Tbit/in<sup>2</sup> Reader Design outlook [3] helps us to understand how to design magnetic read sensor for areal density >1Tbit/in<sup>2</sup>. They found that the reader signal-to-noise ratio (SNR) requirement will be extremely challenging due to the quick increase in noise and the extra requirements from assisted writing. Figure 2.7 shows projected reader noise for a range of recording density, noise projection contains both measurement and calculation. The solid curve shows the thermal magnetic noise, which bends near 1Tbit/in<sup>2</sup>. This is because the noise density values below 1Tbit/in<sup>2</sup> are measurement, the values above 1Tbit/in<sup>2</sup> are calculation results, and the two regions do not exhibit exactly the same rate of change.

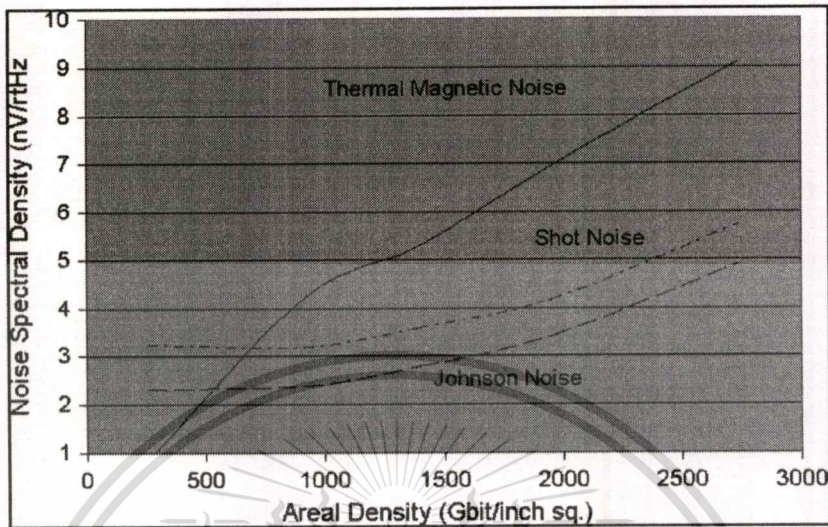


**Figure 2.7** Projected reader noise for a range of recording density. [3]

An acceptable level of channel bit density can be achieved in spite of a calculated head-to-media spacing (HMS) decrease provided that both the shield-to-shield (SS) spacing the scale down of bit length. They expected the side reading control for high KTPI to be complicated, and potentially a reader side shield will be necessary. The reader will likely use a higher quality MgO (barrier) tunneling magnetoresistance (TMR) stack with improved permanent-magnet coercivity. Certain new structures such as the differential reader or the tri-layer will likely be part of the resolution.

In [4] paper, Magnetoresistance Ratio and Resistance Area Design of CPP-MR Film for 2-5Tbit/in<sup>2</sup> Read Sensors, they estimated the CPP-GMR performance goal required for hard disk drives with areal density from 2 to 5Tbit/in<sup>2</sup>, allowing for spin transfer torque (STT) and thermal magnetic noise. They found that the noise due to STT considerably affects the MR performance target for low resistance area (RA) film. Magnetic read sensor with higher RA (about 0.1-0.3Ω.μm<sup>2</sup>) is preferable to control STT. In addition, thermal magnetic noise remained smaller than media magnetic noise for 2Tbit/in<sup>2</sup> while it becomes comparable to media magnetic noise for 5Tbit/in<sup>2</sup>, suggesting the essential of a new method to control thermal magnetic noise.

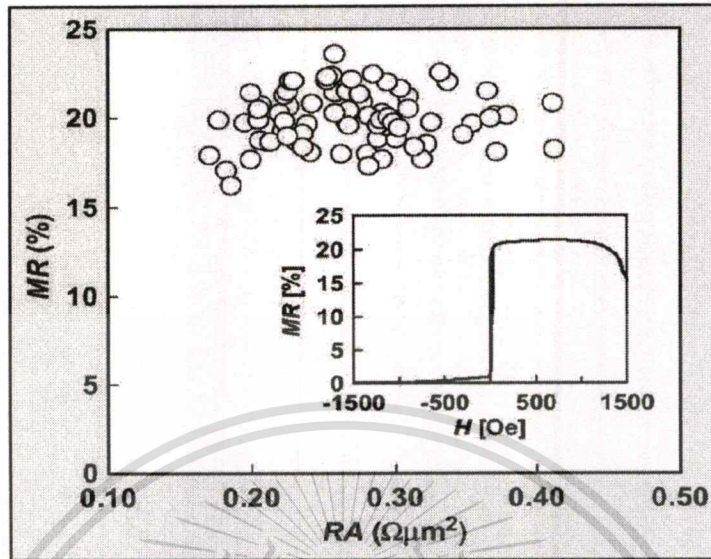
**Table 2.1** Simulation condition [4]

| Areal Density (AD)                            | 2Tbit/in <sup>2</sup> | 5Tbit/in <sup>2</sup><br>(w/o SS) | 5Tbit/in <sup>2</sup><br>(with SS) |
|---|-----------------------|-----------------------------------|------------------------------------|
| Bit Aspect Ratio                              | 3                     | 1.6                               | 1.6                                |
| TPI (KTPI)                                    | 816                   | 1768                              | 1768                               |
| BPI (KBPI)                                    | 2450                  | 2828                              | 2828                               |
| Track pitch                                   | 31.1nm                | 14.4nm                            | 14.4nm                             |
| Magnetic Clearance                            | 5nm                   | 4nm                               | 4nm                                |
| Physical element width<br>(simulation result) | 21nm                  | 10.5nm                            | 10.5nm                             |
| Stripe height                                 | 21nm                  | 10.5nm                            | 10.5nm                             |
| Read gap (simulation result)                  | 20nm                  | 13.5nm,                           | 13.5nm,                            |

In [7] CPP-GMR Film with ZnO-Based Novel Spacer for Future High-Density Magnetic Recording, they study new type of CPP-GMR sensor, which has ZnO-based novel spacer. A high MR ratio of 21.4% at of about  $0.2 \Omega \cdot \mu\text{m}^2$  at room temperature was obtained by optimization of the fabrication condition of ZnO layer.

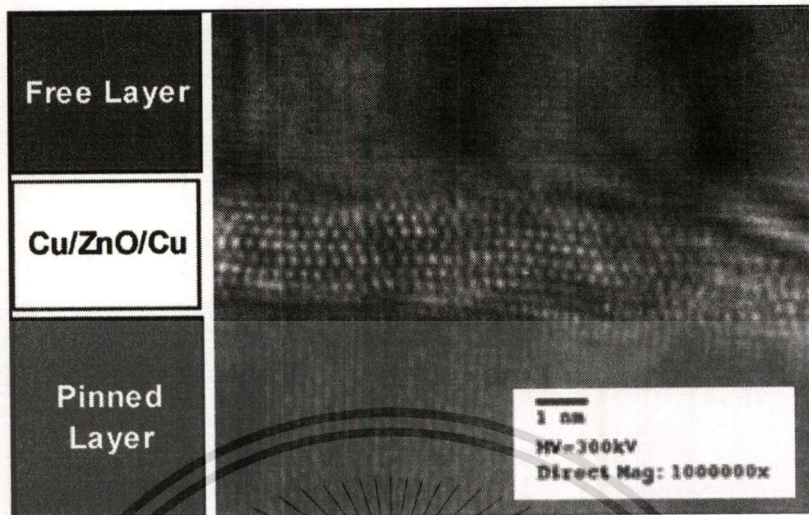
Figure 2.8 shows a high MR ratio of 21.4% at of about 0.2 at room temperature was obtained. The obtained QST curve suggests the very small coercive force of free layer and good robustness of pinned layer, which are suitable for HDD head application.

Figure 2.9 shows the cross-sectional high-resolution transmission electron microscopic (HRTEM) image enlarged near novel spacer region of CPP-GMR film. The spacer configuration is Cu/ZnO/Cu. Although it is difficult to detect the interface of ZnO/Cu accurately, the ZnO-based spacer is crystalline which have c-axis orientation with wurtzite structure, and there are no metallic portions, which are generally observed in CCP type CPP-GMR.



**Figure 2.8** MR ratio dependence on RA [7]

Based on HRTEM observation, the ZnO spacer is crystalline which have c-axis orientation with wurtzite structure, and there are no metallic portions. The measured noise is in excellent agreement with Johnson noise fitted at  $T=400$  K. This result suggested that the contact at ZnO-based spacer interface with magnetic electrode is ohmic. First principle calculations that used a simple model supported the existence of large spin dependent scattering at the interface of ZnO layer. These results indicated that higher signal to noise ratio can be achieved in this type of CPP-GMR head even with lower MR ratio than MTJ (magnetic tunneling junction) sensor and it is very attractive candidate of future magnetic read sensor in HDDs.



**Figure 2.9** Cross sectional HRTEM of CPP-GMR film. [7]

In [8] CPP-GMR Heads with a Current Screen Layer for 300Gbit/in<sup>2</sup> Recording, They studied CPP-GMR with a current screen layer were fabricated, and the recording performance was measured. Output voltages or sensitivity of 1.9 mV and signal-to-noise ratio (SNR) of about 30 dB were obtained from a 50nm track width with an operating voltage (volt bias) of 120 mV. The MR ratio was 4%-5%, shield to shield spacing was 36 nm and resistance was 72 $\Omega$  with using the thermal fly-height control. The fabricated sensor showed a potential to yield a 382Gbit/in<sup>2</sup> recording (1252 kBPI x 305 kTPI). The current screen structure condensed the spin torque noise since just a low sensing current of 1-2mA was required for obtaining a high output. Recently developed CPP-GMR sensor showed the MR ratio of 18%-19% with the RA product of 0.2-0.3  $\Omega \cdot \mu\text{m}^2$ .

Computation allowed the magnetic read sensor achieve 30 dB or more in SNR when track width was 40 nm or larger. The current screen CPP-GMR sensor showed high potential for an areal density of >500Gbit/in<sup>2</sup>.

Figure 2.10 shows the head-amp SNR as a function of the sensor width for three kinds of the heads described above. Head-amp SNR decreased monotonically with decreasing the sensor width for the current screen and TMR heads. This was due to a large bandwidth and a large head resistance from a narrow track. The SNR of the all metal heads had a peak around the sensor width of 40 nm.

The reason for the low SNR for the wide track region was the large spin torque noise. The sensor width was 100 nm or wider, the TMR and current screen heads showed almost same SNR. When the width was between 40 and 100 nm, the current screen heads showed the best SNR of 30 dB or more. Thus, the current screen CPP-GMR head is an attractive candidate that has a high potential suitable for an areal density of 500 Gb/in<sup>2</sup> or more. Beyond that point with the sensor width of 40 nm or less, the all metal head would be the best candidate. We have a chance simply to remove the screen layer to make the current screen CPP-GMR film all metallic. The largest noise source would be the magnetic noise, since the sensor volume becomes very small.

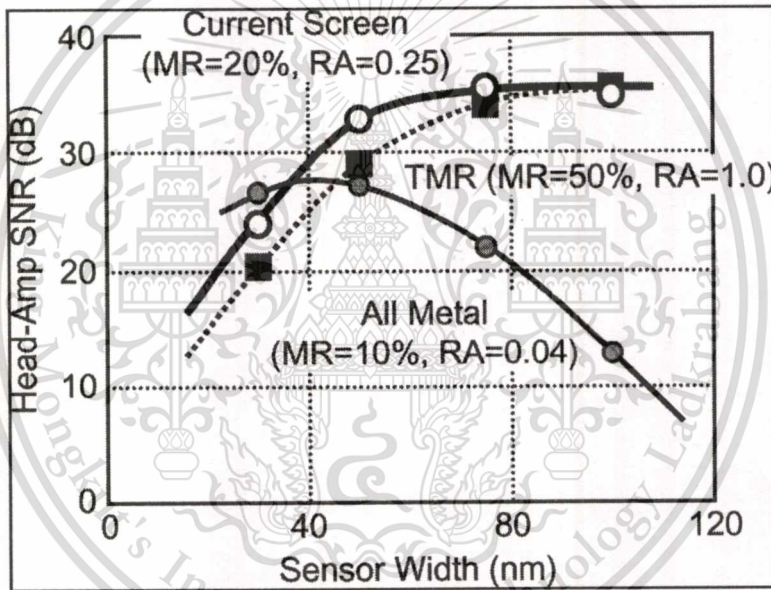


Figure 2.10 Calculated SNR versus sensor width for three kinds of reader. [8]

### 2.3 CPP-GMR technology opportunity

There are two papers are reviewed in this groups, why CPP-GMR show an opportunity to be new candidate in high areal density. There are two important criteria they we need to select CPP-GMR instead of TMR.

CPP-GMR has attracted much attention due to its lower resistance area product (RA) than TMR which is more favorable for magnetic read sensor application in terms of high frequency and

low noise. It is necessary to achieve RA less than  $0.2\Omega\mu\text{m}^2$  in order to adapt to the recording density up to  $2\text{-}3\text{Tbit/in}^2$ . The recording density increase to  $2\text{-}3\text{Tbit/in}^2$ , the high frequency response of magnetic read sensor is required. CPP-GMR has a potential for a high MR ratio with an appropriate resistance. Magnetic read sensor resistance can be in a range of  $50\text{-}200\text{ohm}$ , which is suitable for high data transfer rate. Although TMR sensors are currently the main read head, head resistance without an external field becomes up to  $500\text{-}600\text{ohm}$  when the sensor size becomes small down.

Resistance area product (RA) in unit of  $\Omega\mu\text{m}^2$ , the RA will be decreased when areal density increase. In order to increase the data transfer rate for higher areal density recording the RA of magnetic read sensor must be reduced. These trends indicate that the TMR sensor, whose minimum achievable RA value is thought to be about  $1\Omega\mu\text{m}^2$ , will face the RA limit at about  $300\text{Gbit/in}^2$ .

In [9] CPP-GMR Technology for Future High-Density Magnetic Recording, They have enhanced the CPP magnetoresistance of fully metallic spin-values by developing two groups of new magnetic materials for each magnetic layer. The first groups are spin-blocking materials that control the spin-dependent transport through the synthetic ferrimagnet pinned layer using impurities. Pinned layers of these new materials do not have the low magnetoresistance disadvantage of the synthetic pinned layer in CPP spin valves. The other groups are high-resistivity magnetoresistive materials that contain a relatively high resistivity metal and have spin-dependent scatterings. These materials expand the possibility of improving the output of the CPP-GMR, which has a small resistance, and signal to noise ratio, and low resistance are required in read sensors for high-density recording and fast data transfer, CPP-GMR technology will be indispensable for the future system of high density magnetic recording.

Figure 2.11 shows the trends of data transfer rate for high-end hard disk drive systems and allowed resistance-area product (RA) of read head sensors with a current perpendicular to plan (CPP) structure versus areal density. As can be seen the RA of CPP sensor must be reduced in order to increase the data transfer rate for higher areal density recording. These trends indicate that the TMR sensor, whose minimum achievable RA value is thought to be about  $1\Omega\mu\text{m}^2$ , will face the RA limit at about  $300\text{Gbit/in}^2$ .

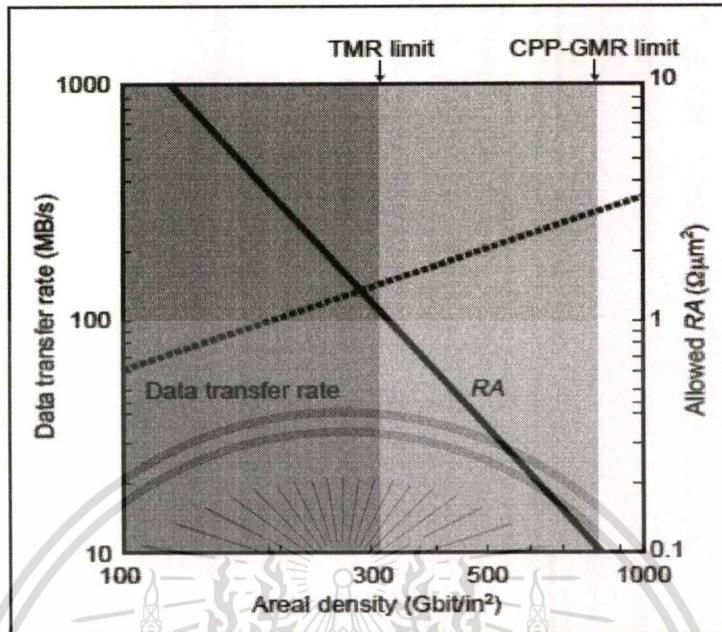


**Figure 2.11** Trends of data transfer rate for high-eng HDD systems and allowed RA with CPP structure versus areal density [9]

However, the performance of CPP-GMR sensors that use spin-valves made of conventional materials is limited by their less than  $1\text{m}\Omega\mu\text{m}^2$ . This value is small because of the small change in film resistance that occurs when the relative angle between magnetizations of two magnetic layer materials is changed. The moderate intrinsic magnetoresistance value and the minimum CPP resistance of spin-valves results in a  $\Delta\text{RA}$  that is very small to achieve a sufficiently high signal to noise ratio (SNR).

In [10] CPP-GMR technology for magnetic read heads of future high-density recording systems, This paper introduced CPP-GMR technology, features, routes to output development, issues to be solved and possibilities as a magnetic read sensor. For example, use of high spin-dependent bulk scattering, high resistivity or half-metallic magnetic materials for free layer and reference magnetic layers were shown as ways to improve the output of CPP-GMR. A current state of CPP-GMR sensor enlargement was also mentioned in view points of sensor downsizing, magnetic head noise and high density recording revelation. CPP-GMR still has some points to be improved; however it is believed

that the CPP-GMR will actualize a next high-performance magnetic read sensor in no distant future.

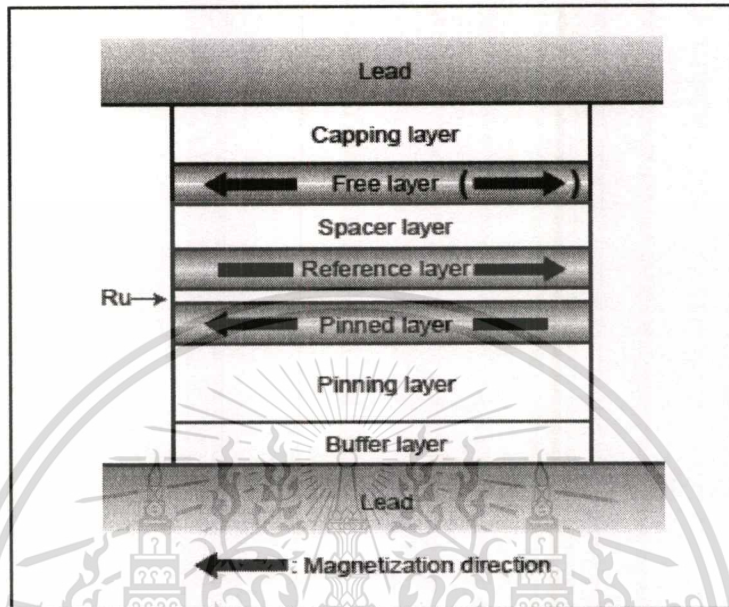


Figure 2.12 CPP-GMR structure used for calculating  $\Delta RA$  [9]

## 2.4 Principle and Theory of Magnetic Read Sensor

There are three papers are reviewed in this groups, magnetic read sensor is very sensitive and critical technology. We need to understand the standard component of magnetic read sensor for both TMR and CPP-GMR and important parameters in term of designs for both magnetic properties and physical dimensions. In order to achieve high areal density, we need to consider not only how to design the magnetic read sensor but also how to process the sensor as per designed. The performance and reliability of magnetic read sensor can measure by static and dynamic test in term of only magnetic recording head and all HDD systems.

In [5] Magnetic recording read head sensor technology, they present that they can detect and transmit information from recorded data at areal density  $>200 \text{ Gbit/in}^2$  and data rates approaching 1GHz, several advances in nano-magnetic, magnetic ultrathin films, magneto-electronics, as well as device processing, has remarkable progress of this technology. They present an overview of the

science and technology behind magnetic read sensor.

The dimension, geometry and magnetic requirements for the read sensor are described, followed by a description of the state of the art giant-magnetoresistive read sensors. Then they discussed characteristics and potential advantages of next generation magnetic read sensors, including current-perpendicular-to-plane tunneling magnetoresistance (TMR) and giant magnetoresistive sensors (CPP-GMR). The interaction between sensor properties, size necessities, process restrictions and magnetic read sensor performance is emphasized.

**Table 2.2** Representative dimensions of the recording system for a HDD product with areal density of 80Gbit/in<sup>2</sup>

| Attribute system      | Value                   |
|-----------------------|-------------------------|
| Areal density         | 80 Gbit/in <sup>2</sup> |
| Tracks per Inch (TPI) | 100,000/in <sup>2</sup> |
| Bits per Inch (BPI)   | 800,000/in <sup>2</sup> |
| Attribute-transducer  |                         |
| Write width           | 200 nm                  |
| Read width            | 120 nm                  |
| Guard band width      | 40 nm                   |
| Shield separation     | 60 nm                   |
| Track pitch           | 240 nm                  |
| Bit length            | 30 nm                   |

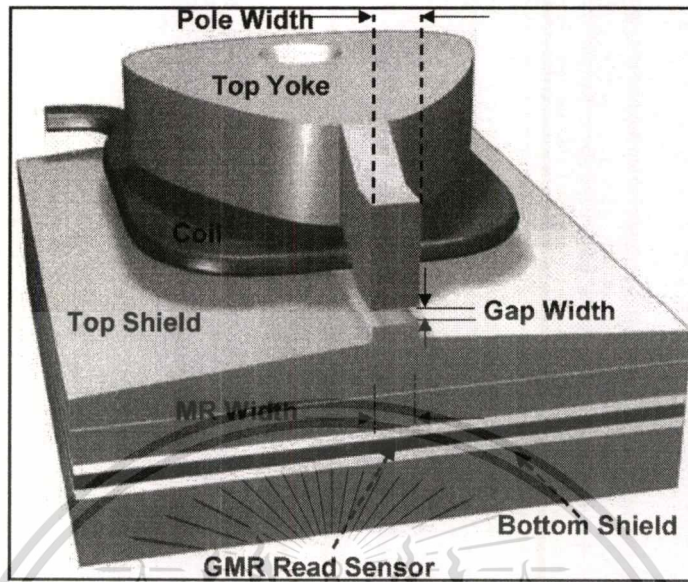


Figure 2.13 Thin-film head structure as viewed from the media disk surface. [5]

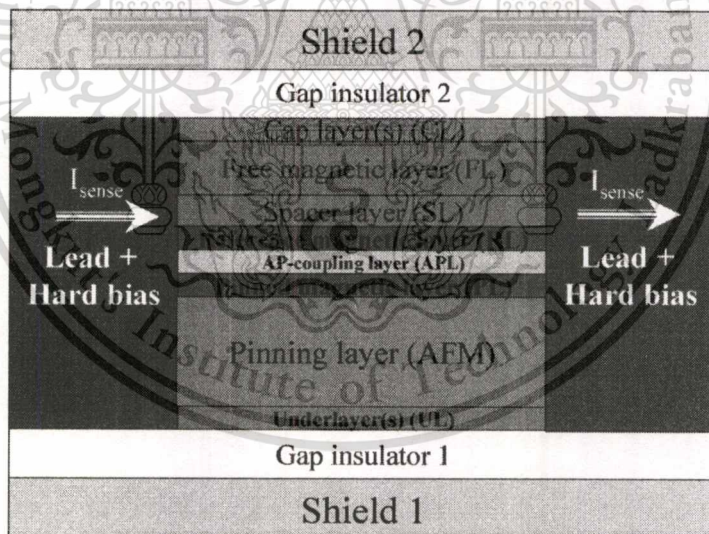
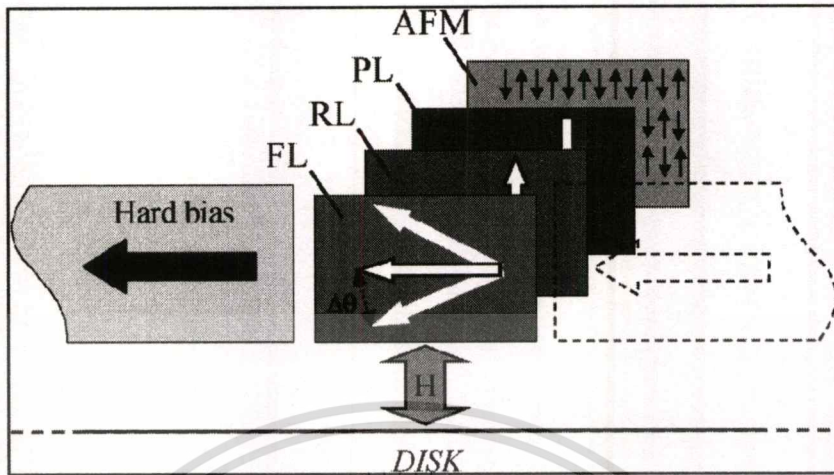


Figure 2.14 Disk-view schematic of CIP GMR sensor. [5]



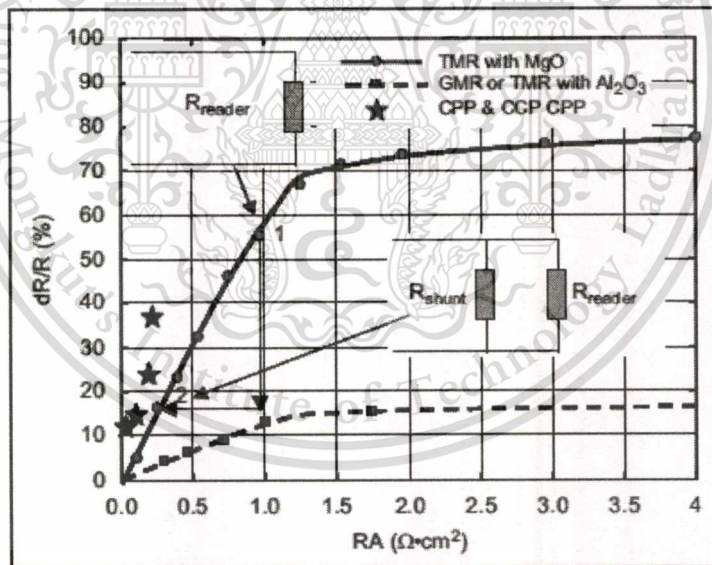
**Figure 2.15** Signal transition fields from the recorded media for TMR or CPP-GMR. [5]

Figure 2.15 shows perspective view of the relative magnetization directions of the Hard bias, free sensing layer (FL), reference layer (RL), pinned layer (PL), and pinning anti-ferromagnetic layer (AFM) for a typical GMR head. The signal transition fields  $H$  from the recorded media disk are oriented vertically. These relative orientations also apply to CPP-TMR or CPP-GMR heads.

In [6] Read and write processes, and head technology for perpendicular recording, this paper presents a review of the write and read processes in perpendicular magnetic recording. They discussed their impact also, based on recording physics aspects, on design considerations for writers and readers head. For the write process, they discuss fundamental write-ability restrictions as well as possible paths to ultra-high areal density perpendicular recording. The impacts of different medium designs, geometrical scaling, and the breakdown of scaling, both in terms of write-ability and evolution curvature, are shown based on different modeling techniques, including analytical formulas, finite element modeling (FEM), and micromagnetic simulations. Not only basic design policy but also alternative designs that permit high areal density are briefly explained. In term of read-back process, the relation between reader signal to noise ratio (SNR) and resistance, as well as reader resistance shunt and spacing loss, are discussed. Finally, they use a simple example to demonstrate, both from a write as well as a read back perspective, the complicated nature of perpendicular recording systems, and how different medium designs impact recording head technology for ultra

high density perpendicular recording.

The read sensors in current magnetic recording hard disk drives are based on tunneling magnetoresistance. The usable TMR ratio vs. reader resistance area product (RA) typically follows curves such as the one shown in Figure 2.16 (solid line). For a small value of RA, the potential TMR ratio, and therefore reader amplitude, is proportional to RA. At larger RA, the amplitude cannot increase linearly with RA and saturates at some value. The saturation value depends on the barrier material and process conditions; MgO reader have higher  $\Delta R/R$  value than typical  $\text{Al}_2\text{O}_3$  barriers. If we assume that the electronic noise (Johnson/shot noise) only depends on reader resistance and that the thermal magnetic noise is the same for similar dimensions of the reader, then the MgO reader will have much higher SNR than other TMR heads due to its much higher value of  $\Delta R/R$  for a given RA. In reality, since thermal magnetic noise also scales with  $\Delta R/R$ , the total SNR gain from MgO reader due to amplitude gains will be reduced.



**Figure 2.16**  $\Delta R/R$  (%) vs. RA for CPP-GMR and TMR. [6]

In [13] Nano Processing Strategies for MR Sensor Read Width and Stripe Height Formation, They study how to process the MR sensor when the areal increases  $>100 \text{ Gbit/in}^2$ . The critical dimensions of recording heads continue to scale down at a rate of 15%-30% per year. Magnetic read sensors with 100nm physical read track widths are being normally fabricated using undercut resist images and solvent based liftoff processes. However, because standard liftoff processes using undercut photo resist images have reached their limits and cannot be performed reliably below 100 nm, sensor stabilization with a hard magnet adjacent junction is compromised because of induced variations in junction profile and hard magnet geometry.

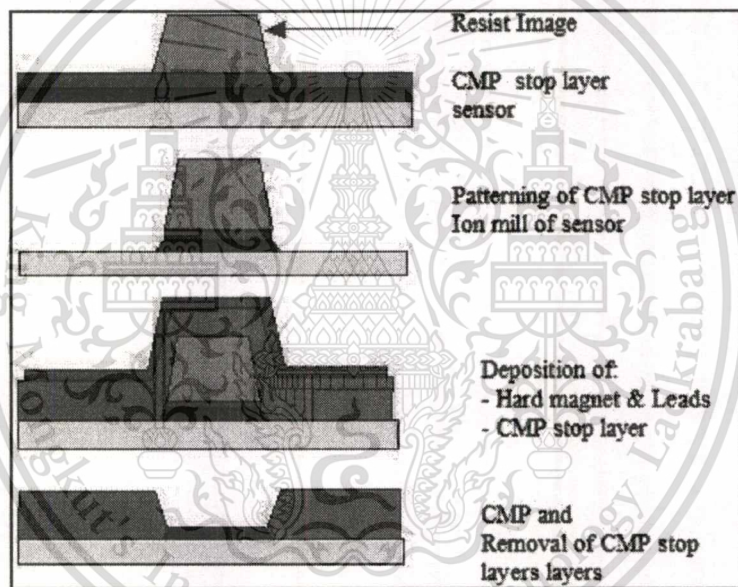


**Figure 2.17** Read width definition using CMP-based liftoff process. [13]

Moreover, an alternative sensor patterning approach is proposed based on chemical mechanical polishing (CMP) and no-undercut resist images to define the read sensors critical dimensions. Ultra narrow giant magnetoresistive (GMR) read heads have been effectively fabricated with physical read track widths in the 20-80nm range and using various sensor designs, Current in-plane (CIP) GMR, current perpendicular to the plane (CPP) GMR, and CPP tunnel magnetoresistive (CPP-TMR) sensors.

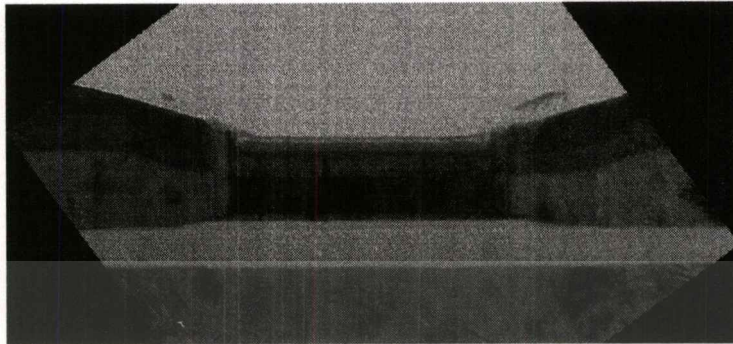


**Figure 2.18** ABS TEM cross section of a 90 nm wide CIP GMR read sensor. [13]



**Figure 2.19** ABS TEM cross section of a 95 nm TMR read sensor. [13]

Table 2.3 projects the critical thickness and lateral read width requirements for the read sensors in year 2010 according to three scenarios and a BAR decrease of 10% per year. Scenario A corresponds to a 70% density growth equivalent to a 27% decrease in feature size; scenario B corresponds to a 40% growth equivalent to a 20% reduction of feature size; and finally, scenario C to a 30% density growth with a 17% decrease in feature size. It is shown that by 2010, read gaps and track widths smaller than 36 nm may be necessary to satisfy the density growth requirements. One can envision that the read gaps requirements could be met with thin CPP or TMR sensors since they do not require additional dielectric gaps, but the patterning processes will face significant challenges. To study process extend ability, e-beam defined resist lines as small as 20 nm have been printed on wafers coated with sensor material.

**Table 2.3** Critical thickness and Lateral, Read width Requirements in Year2010 [13]

| Scenario | Areal Density             | BAR | MR Gap | MR track width |
|----------|---------------------------|-----|--------|----------------|
| 2006     | 125 Gbit/in <sup>2</sup>  | 8.0 | 50nm   | 100nm          |
| A-2010   | 1045 Gbit/in <sup>2</sup> | 5.2 | 22nm   | 29nm           |
| B-2010   | 480 Gbit/in <sup>2</sup>  | 5.2 | 32nm   | 41nm           |
| C-2010   | 360 Gbit/in <sup>2</sup>  | 5.2 | 36nm   | 47nm           |

## 2.5 Characteristics and Reliability study for Magnetic Read Sensor

There are four papers that we reviewed in term of characteristic and reliability for magnetic read sensor, Magnetic read sensor characteristic and reliability can studied by quasi static test (QST) and dynamic electrical tester (DET). Electrostatic Discharge (ESD), Temperature and volt bias dependence are very important for both magnetic read sensor TMR and GMR sensors, even the degradation detail is different. ESD, temperature and volt dependence can tell us the property of spacer or barrier of magnetic sensor, MR ratios decrease drastically with increasing temperature and volt bias.

In [11] Characteristics of Electrostatic Discharge Induced Damage on Magnetic Tunnel Junctions, They investigated electrostatic discharge (ESD) sensitivity of current perpendicular to plane (CPP) magnetic tunnel junctions (MTJ) used in hard disk drives (HDD). The recent generations of HDDs increasingly use MTJs while the current in plane (CIP) giant magnetoresistive (GMR) heads are being slowly phased out. They have found that, in general, the ESD sensitivity of CPP-TMR and CIP-GMR sensors is comparable at the same areal density point. The difference is in the details of degradation. With increasing ESD voltage pulse applied across the two junctions of the magnetic sensor, the amplitude of a GMR reader degrades first, while resistance remains stable to higher ESD voltage levels and finally increases. With the TMR sensor is that resistance decreases first, while the amplitude still stable to higher ESD voltage levels and finally decreases.

They also investigated the instability generation in TMR with increasing ESD levels. They described the experimental method, recorded the observations, and analyzed them to understand the source of instability.

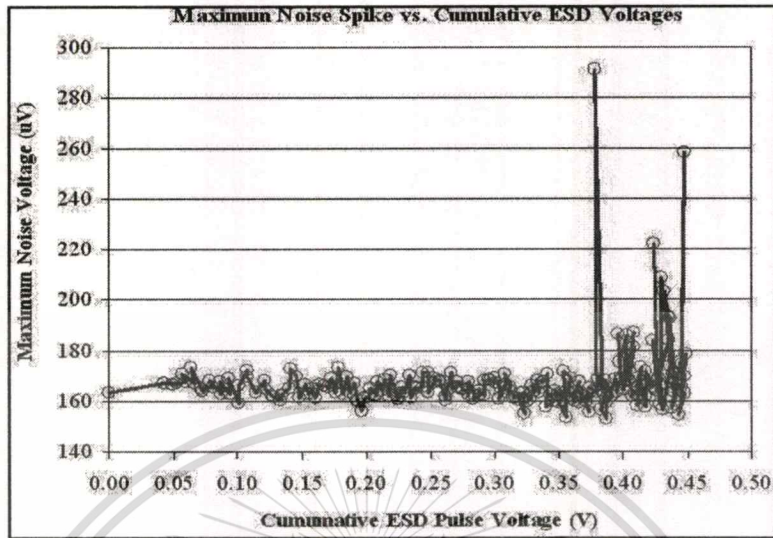


**Figure 2.20** High frequency noise spikes could be induced as well as be cured  
By cumulative ESD pulses for MTJ readers [11]

In [12] Temperature and bias-voltage dependences of tunneling magnetoresistance in Ga,Mn As based double barrier magnetic tunnel junctions, They investigated the temperature and bias voltage dependences in the tunneling magnetoresistance (TMR) curves for Ga,Mn as-based double-barrier magnetic tunnel junctions (DB MTJs). The coercive fields in each magnetic Ga,Mn as layer significantly decrease depending on the variations in the temperature. TMR ratios decrease drastically with increasing temperature. Moreover, they have demonstrated that DB MTJs not only improve the TMR ratio effectively but also develop the strong bias voltage characteristics.

Figure 2.21 shows TMR curves for the DB MTJs that depend on the measurement temperature. The TMR curves were obtained by sweeping the magnetic field from the positive maximum at 0.6 kG to the negative maximum at  $-0.6$  kG and vice versa. TMR ratio as a function of the magnetic field ( $H$ ) is defined as  $MR(H)=[R(H)-R_p/R_p]$ , which is measured at a constant current of 100 nA.

Multi terraced structures are derived from various magnetic configurations of three magnetic layers, which originate from the effects of the DB structures due to the difference in the coercive field ( $H_c$ ) in each (Ga,Mn)As layer since the  $H_c$  and  $TC$  depend on the layer thickness.

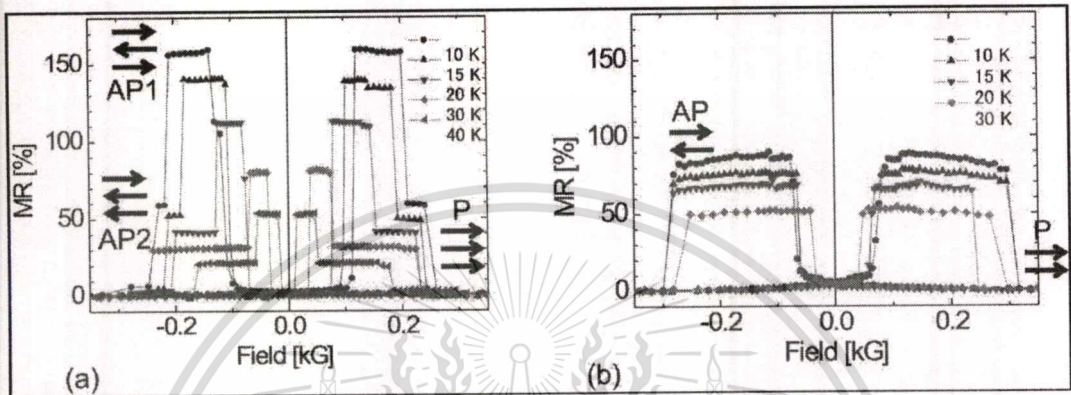


**Figure 2.21** Variations in TMR curves with temperature.

a) DB MTJ and b) SB MTJ [12]

The temperature dependence for SB MTJ is also plotted as the open markers.  $H_c$  of the magnetic free layer decreases with temperature while that of the magnetic pinned layer remains almost unchanged.  $H_c$ 's of the top magnetic layers in both DB- and SB MTJs remain constant with increasing temperature. This is due to the annealing effects during the device processing, which increases  $TC$  and  $H_c$ 's of only the top magnetic (Ga,Mn)As layer. On the other hand, TMR ratios decrease linearly and similarly as a function of the temperature, as shown in Figure 2.22, for both SB and DB MTJs.

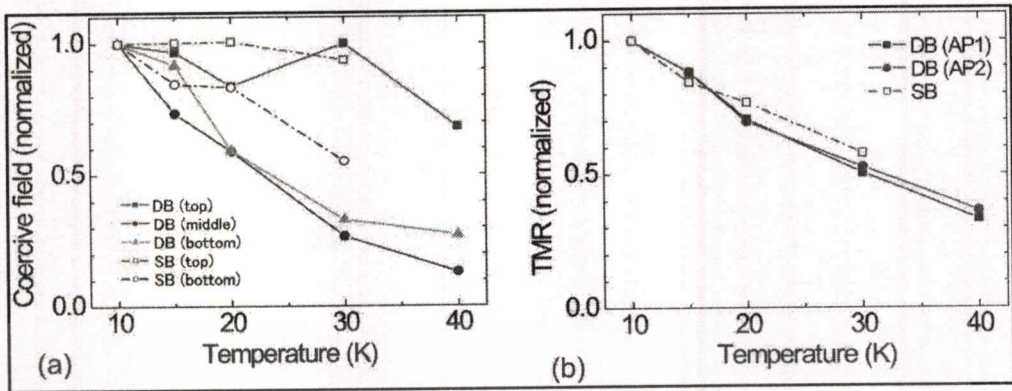


**Figure 2.22** Temperature dependence of a) the coercive field for each layer and b) TMR curves for DB MTJ and SB MTJ. [12]

Figure 2.23 shows the bias-voltage dependence of the TMR ratios for both DB and SB MTJs at 10 K. When the bias voltage is increased, the TMRs decrease for both cases. Almost symmetric line shapes are obtained for the bias voltage.  $V_{\text{half}}$  in DB MTJs and SB MTJs are estimated to be approximately 0.17V and 0.06V, respectively. The enhancement of the  $V_{\text{half}}$  in the DB MTJ cannot be explained by assuming that the externally applied bias voltage is divided by two SB MTJs.

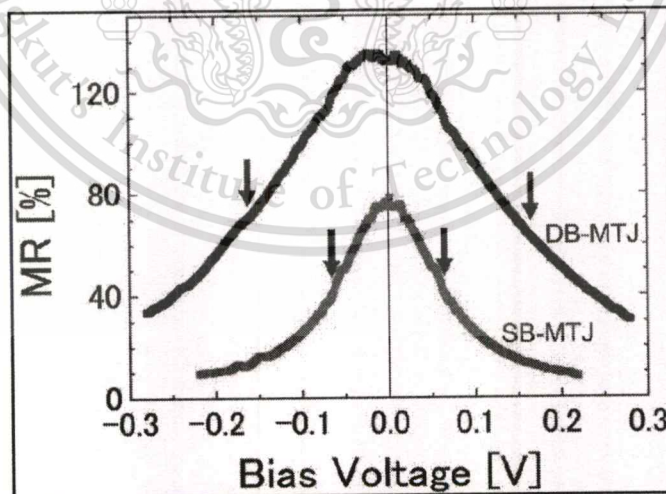


**Figure 2.23** Bias voltage dependence of TMR for DB MTJ and SB MTJ. [12]

In [14] Commercial TMR Heads for Hard Disk Drives: Characterization and Extendibility At 300 Gbit/in<sup>2</sup>, They studied Tunneling magnetoresistive (TMR) reading heads at an areal density of 80-100 Gbit/in<sup>2</sup> in a longitudinal magnetic recording (LMR). The first generation TMR sensors utilized a bottom TMR stack and an abutted hard bias design. These TMR sensors have confirmed three times the amplitude of comparable giant magnetoresistive (GMR) devices, resulting in a 0.6decade bit error rate gain over GMR. This has enabled high component and drive yields. Due to the improved thermal dissipation of current perpendicular to plane geometry (CPP), TMR sensor performs better and has better lifetime performance, and has demonstrated the similar electrical static discharge robustness compared to GMR. TMR has demonstrated equivalent or better process and wafer yields compared to GMR in current in plane geometry (CIP-GMR). The TMR sensor is proven to be a mature and capable magnetic reader technology. Using the same TMR head design in conjunction with perpendicular recording system (PMR), 274 Gbit/in<sup>2</sup> has been demonstrated. Further design can achieve 311 Gbit/in<sup>2</sup>.

In [15] Spintronics: Fundamentals and applications, this article reviews the current status of this subject, including both recent advances and well established outcome. The primary focus is on the basic physical principles fundamental the generation of carrier spin polarization, spin dynamics, and spin-polarized transport in semiconductors and metals. Spin transport differs from charge transport in that spin is a non-conserved quantity in solids due to spin-orbit and hyperfine coupling. The authors discussed in detail about spin de-coherence mechanisms in metals and semiconductors.

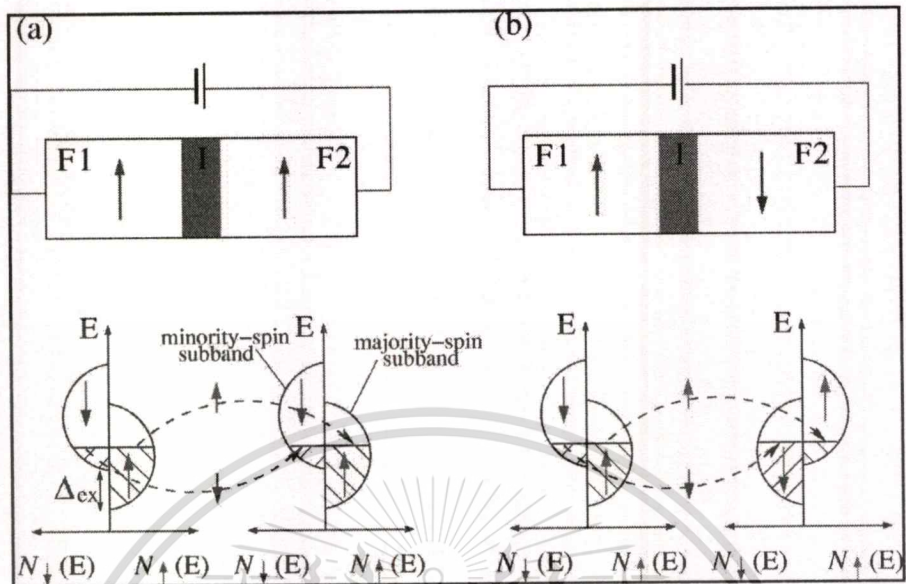


**Figure 2.24** Schematic illustration of electron tunneling in ferromagnet / insulator / ferromagnet  
(a) Parallel and (b) anti-parallel orientation [15]

Various theories of spin injection and spin polarized transport are applied to hybrid structures related to spin-based devices and fundamental studies of materials properties. Experimental work is reviewed with the emphasis on projected applications, in which external electric and magnetic fields and enlightenment by light will be used to control spin and charge dynamics to create new functionalities not feasible or unsuccessful with conventional electronics.

## 2.6 Conclusion

In this chapter, previous and recent studies on the CPP-GMR and TMR sensors have been reviewed. Previous studies are really useful in understanding principles and current issues of the CPP-GMR and TMR sensors. The key performance for magnetic read sensor such as Resistance, Amplitude and SNR performances are studied and described. The physical dimensions of magnetic read sensor against areal density are discussed based on theoretical simulation and experiment, it is observed that the CPP-GMR show high potential to achieve higher areal density with scale down reader size / dimension. The most discouraging challenge for future magnetic read sensor technology

will be thermal activated magnetic noise at small dimensions of track width (TW), shield to shield spacing (SS) and stripe height (SH), which will limit the minimum practical ferromagnetic sensor volume, or necessitate a transition to non-magnetic sensor technologies.



This material is reserved for educational use only, not allowed for commercial use.

Forbidden to modify the content, and cite the document when use.

## CHAPTER 3

# RESEARCH METHODOLOGY

CPP-GMR is the latest magnetic read sensor with all metallic layers instead of TMR which has insulator layers. TMR read sensor has a limit at around  $2\text{Tbit/in}^2$  recording density. Because of its high impedance, we cannot scale down the magnetic read sensor dimensions any further. It is generally accepted that giant magnetoresistance (GMR) reader with all metallic materials and current perpendicular to the plane (CPP) geometry have to be employed in order to achieve areal density  $>2\text{Tbit/in}^2$

Experiments had been performed to study characteristics and reliability of CPP-GMR sensors in order to compare it to current TMR sensors. This is to study possibility of CPP-GMR performance to achieve higher areal density by using quasi static tester (QST). CPP-GMR and TMR sensors were fabricated from WD wafer manufacturing process. We expect that the result of this experiment will be useful for development of future magnetic recording head designs, especially the near future candidate of CPP-GMR sensors.

In chapter 3, there are 5 sections, Section 3.1 is about the concept of slider fabrication process, how to produce magnetic read sensor slider. Section 3.2 describes experiment details. Section 3.3 explains how to characterize performance and reliability of the magnetic read sensor using quasi static tester (QST). Section 3.4 explains detail of reliability test conditions, and finally section 3.5 is the list of materials, testers and research tools used for this study.

### 3.1 Slider Fabrication Process

This section explains Slider Fabricated process (SF process), how to produce magnetic recording head. The current standard process for Western Digital Bang pa-in is shown in figure 3.1 SF process flow. SF Process can be separated to 3 main processes,

#### 3.1.1 Front End process

Front End process starts from wafer loading into strip height grinding, bar dividing then back side lapping operation to get suitable bar thickness and also for stress management. The

most important in this step is MMX or rough lapping and bar level kiss lapping process. The purpose of lapping process is to obtain required stripe height based on target resistance.

### 3.1.2 Clean room process

Clean room process starts from DLC FCA operation, which has the purpose to coat ABS surface with diamond like carbon (DLC) to protect magnetic sensor stripe height. There are 4 steps of Photo Lithography operation to finish clean room process.

### 3.1.3 Back End process

Back End process starts with TIP debond, automate clean, row bond / head part and robot sort then electrical performance measurement at quasi static tester (QST). Finished sliders are separated by Robot sorter as per electrical performance from QST. Then parts are passed through automatic cleaning operation and appearance inspection at air bearing surface (ABS inspection) as final operation.

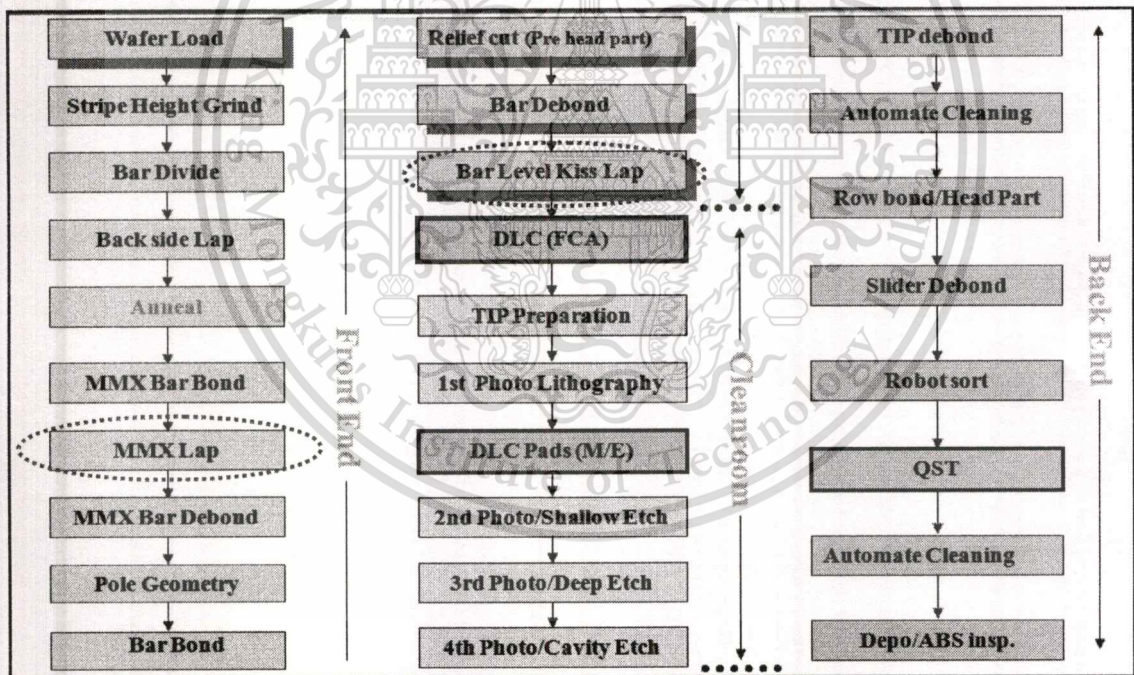
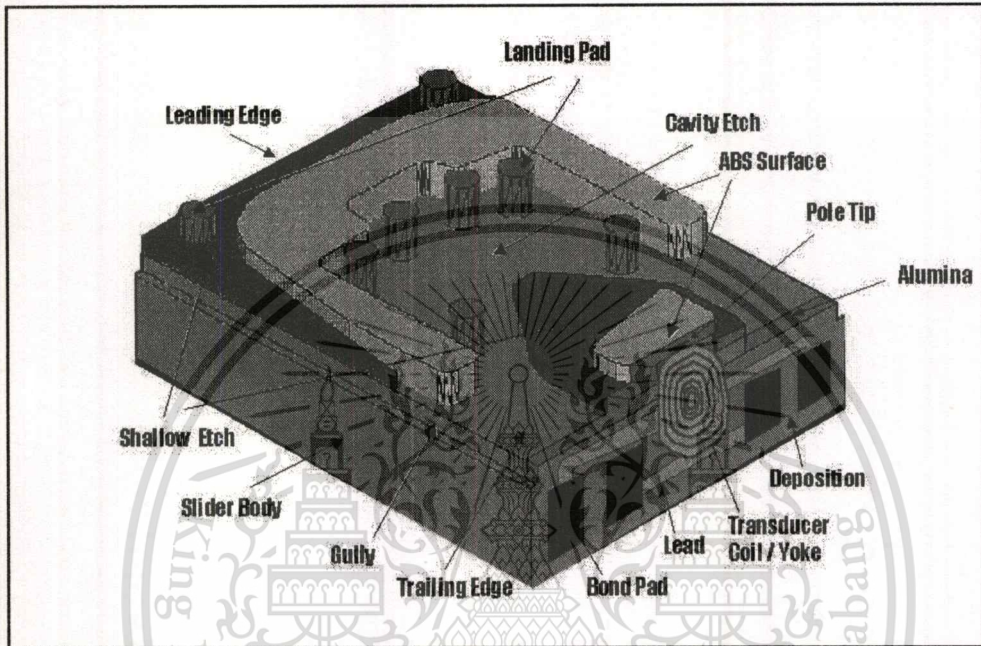
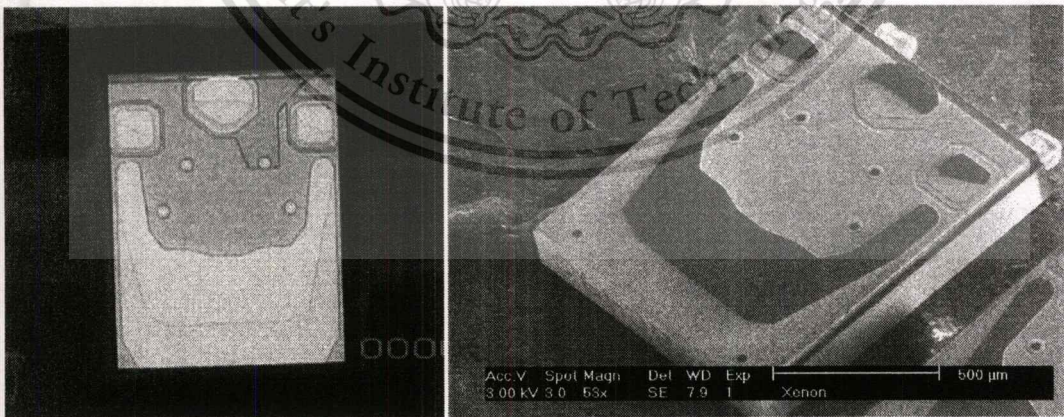


Figure 3.1 Slider fabrication process flow

Figure 3.2 and 3.3 shows finished slider consists of writer or transducer coil and magnetic read sensor connected to bonding pad by a very small lead line at deposition side. ABS surface consists of Landing pads, Landing Edge, Shallow Etch, Cavity Etch and Trailing Edge which are engineered to fly above the disk in nanometer scale.



**Figure 3.2** Slider component



**Figure 3.3** Slider ABS side

### 3.2 Experiment Details

CPP-GMR and TMR sensors were fabricated from WD design team then finish slider fabricate process at WD Bang pa-in. We performed experiment per below steps;

3.2.1 Select magnetic read sensor CPP-GMR and TMR with same areal density, same read track width and same magnetic material but different spacer of CPP-GMR and barrier of TMR sensor. In this study CPP-GMR is copper (Cu) and TMR is MgO.

3.2.2 Selected CPP-GMR and TMR sensors were processed at slider fabrication at WD Bang pa-in, varying aspect ratio (AR) from 0.4 to 1.6. CPP-GMR.TMR sensors with different AR were processed at MMX lap and bar level kiss lap processes as shown in Figure 3.1. Defined reader electrical lapping guide (ELG) was performed for each AR on both CPP-GMR and TMR sensors. Sample size of each AR is 500-1000 sliders for both CPP-GMR and TMR which are obtained from 4-5 wafers.

**Table 3.1** Stripe height (SH) and Aspect ratio (AR) for CPP-GMR & TMR

| no | CPP-GMR |         |            | TMR     |         |            |
|----|---------|---------|------------|---------|---------|------------|
|    | TW (nm) | SH (nm) | AR = TW/SH | TW (nm) | SH (nm) | AR = TW/SH |
| 1  | 25      | 60      | 0.42       | 30      | 80      | 0.38       |
| 2  | 25      | 50      | 0.50       | 30      | 70      | 0.43       |
| 3  | 25      | 45      | 0.56       | 30      | 60      | 0.50       |
| 4  | 25      | 40      | 0.63       | 30      | 50      | 0.60       |
| 5  | 25      | 35      | 0.71       | 30      | 45      | 0.67       |
| 6  | 25      | 30      | 0.83       | 30      | 40      | 0.75       |
| 7  | 25      | 25      | 1.00       | 30      | 35      | 0.86       |
| 8  | 25      | 20      | 1.25       | 30      | 30      | 1.00       |
| 9  | 25      | 15      | 1.67       | 30      | 20      | 1.50       |

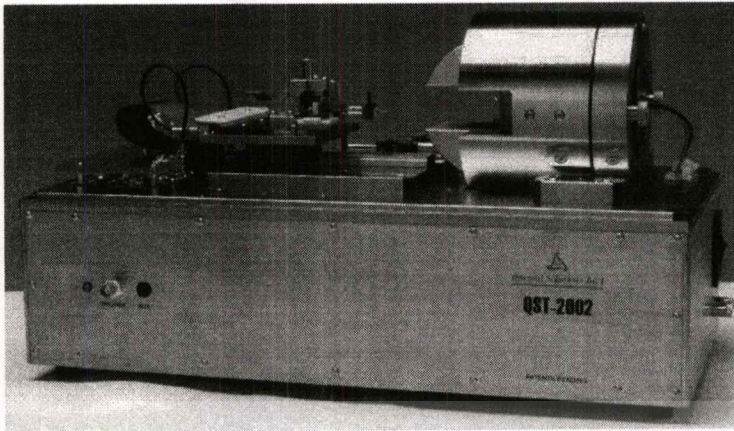


**Figure 3.4** quasi static testers (QST)

In this experiment, we did not finish all slider fabrication process because we want to measure at bar form (54 sliders in one bar) which is easy and suitable for quasi static tester (QST).

3.2.3 Characteristics and reliability study used QST tester. In this experiment we focused on key parameters as follows;

- 1) Resistance (ohm)
- 2) Amplitude ( $\mu\text{V}$ )
- 3) Barkhausen (%)
- 4) Hysteresis (%)
- 5) Static Signal to Noise Ratio - SNR (dB)

There are 2 reliability studies for magnetic read sensor CPP-GMR and TMR.

- 1) Break down voltage (BDV)
- 2) High temperature stress test

### 3.3 Characteristics of Magnetic Read Sensors

The basic characterization of performance and reliability of CPP-GMR were measured using the quasi static tester (QST). QST is test equipment that exposes the read sensor to a uniform external field, which means to simulate the magnetic field from the media on a flying read sensor. In a QST test, a bias current is applied to recording heads, and then the recording head resistance is measured as a function of the external field. The external magnetic field is

swept from negative to positive values, and the obtained resistance versus field curve is referred to as a transfer curve figure 3.5.

Several important magnetic parameters are obtained from the QST transfer curve. There are (1) magnetic read head resistance, measured at a specified bias current, ( $I_{bias}$ ), (2) Amplitude or sensitivity of the sensor, amplitude sometimes refers to zero to peak amplitude and sometimes to peak to peak amplitude. Zero to peak is an average of the negative and positive amplitude from zero to a specified external field. Peak to peak amplitude is the total signal from the negative to the positive applied field.

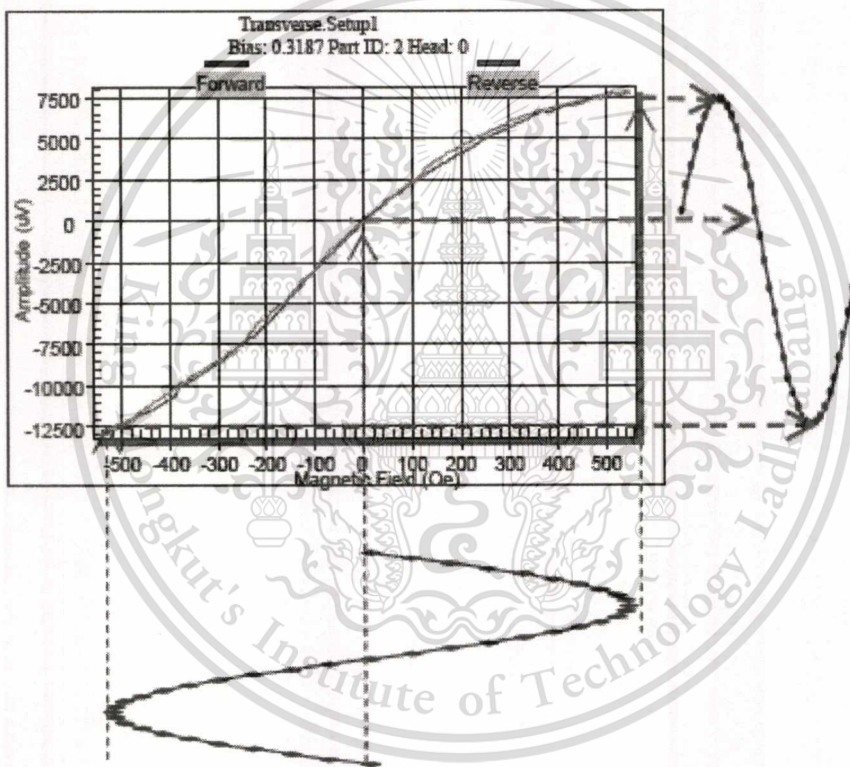


**Figure 3.5** Transfer curve (TC) of Magnetic recording sensor

In this study we also focus on signal to noise ratio (SNR) which is the most important figure of merit for read head performance. Here we refer to static SNR as the SNR measured in a QST tester. The static SNR is defined as  $20 \cdot \log(\text{zero-to-peak QST amplitude} / \text{Noise})$ , where the noise is measured with a bandwidth of 80MHz. The static SNR is a good predictor of the sensor SNR in actual recording conditions on a disk. In order for CPP-GMR sensors to be viable, they need to be equal or exceed the SNR of TMR sensors.

This material is reserved for educational use only, not allowed for commercial use.

Forbidden to modify the content, and cite the document when use.

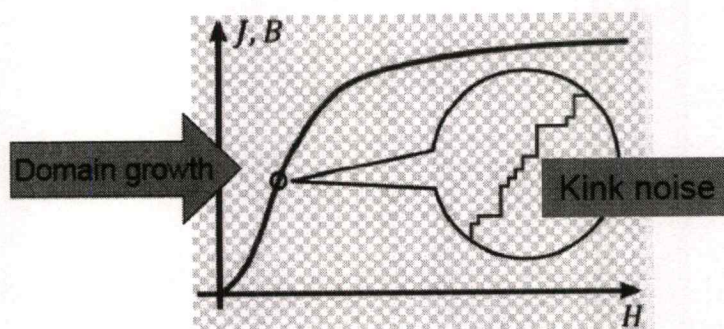


**Figure 3.6** Barkhausen Jump Phenomena of Magnetic Read Sensor

There are 2 stability parameters of magnetic read sensor, (1) Barkhausen Jump (% or  $\mu\text{V}$ ) which is the maximum amplitude jumping between the 2 adjacent samples (measuring points), as show in Figure 3.6. Another is (2) Hysteresis (% or  $\mu\text{V}$ ) which is a measurement area between forward and reverse curves as shown in figure 3.7;

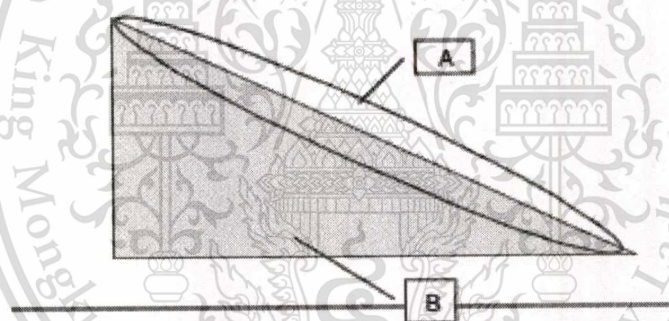


**Figure 3.7** Hysteresis Phenomena of Magnetic Read Sensor

An acceptable magnetic read sensor either CPP-GMR or TMR sensors should have suitable resistance, high sensitivity or amplitude, low Barkhausen, Hysteresis and high static SNR.

To compare static performance of magnetic read sensor CPP-GMR and TMR sensors, same QST measurement conditions were applied for all AR.

- 1) Measurement magnetic field: 520Oe
- 2) Sweep field:  $\pm 520\text{Oe}$
- 3) Volt bias: 140mV

This material is reserved for educational use only, not allowed for commercial use.

Forbidden to modify the content, and cite the document when use.

### 3.4 Reliability test conditions

In this experiment, high temperature stress and break down voltage tests were performed to study reliability of magnetic read sensor. This section explains details of those tests. Only AR 1.0 of both CPP-GMR and TMR sensors were selected to study reliability.

#### 3.4.1 High temperature stress tests

This high temperature stress was generated from dynamic fly height (DFH) portion in magnetic read sensor. Defined volt bias was applied to DFH which has resistance about 105 ohms to generate heat in term of power (mW) then convert to expected temperature as shown in table 3.2. We expect magnetic read sensor which is located beside DFH portion to be heated up when volt bias was applied. We kept bias each step for 120minute to keep the temperature at magnetic read sensor constantly then measured normal QST using normal conditions. Resistance and amplitude changed compared to step1 room temperature was focused.

**Table 3.2** High temperature stress conditions

| step | Stress Power (mW) | High Temperature (°C) |
|------|-------------------|-----------------------|
| 1    | 0.0               | 20                    |
| 2    | 6.7               | 40                    |
| 3    | 10.0              | 50                    |
| 4    | 17.0              | 70                    |
| 5    | 27.0              | 100                   |
| 6    | 34.0              | 120                   |
| 7    | 0.0               | 20                    |

#### 3.4.2 Break Down Voltage stress test (BDV)

We stressed magnetic read sensor by apply voltage starting from 140mV which is standard bias voltage at static QST measurement then increase for 5mV at each step incrementally. BDV point is the voltage that resistance changes equally or more than 30% compared to starting point. Break down point was defined at  $\geq 30\%$  resistance drop due to the barrier or spacer broken from high voltage stress.

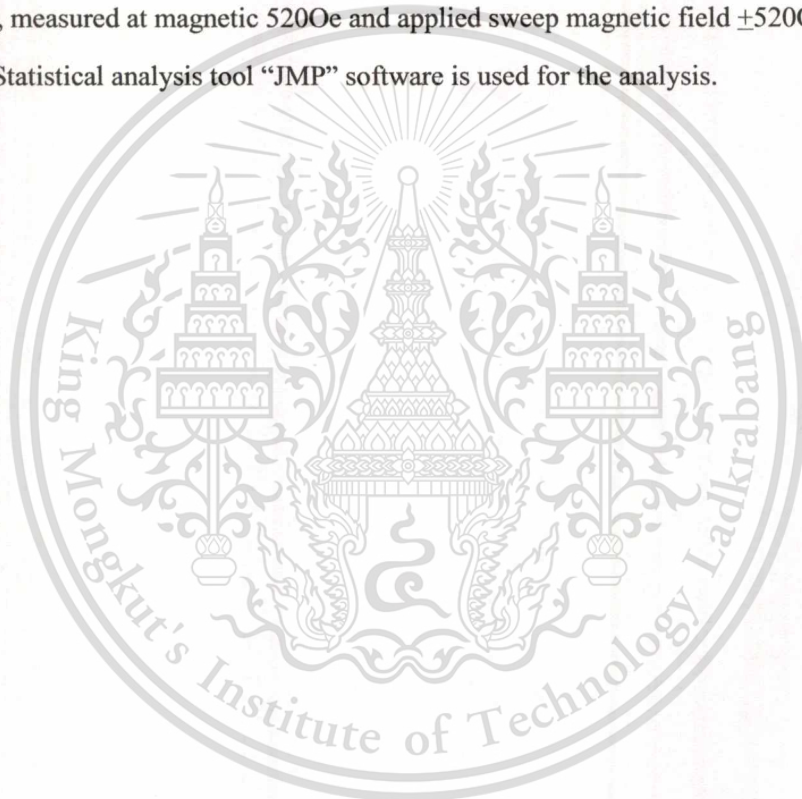
### 3.4 List of Materials and Research tools

Following is a list of materials and research tools that were used to perform the experiment of this thesis.

3.4.1 Magnetic read sensor CPP-GMR and TMR which lapped to met the AR varying from 0.4 to 1.6 in step of 0.3. Each AR has 500 to 1000 heads. The tested head samples were all fabricated using the current Slider Fabrication manufacturing process.

3.4.2 Commercially available quasi static tester (QST) version 2002 and ISI software to setup the measurement condition. Characteristic of CPP-GMR sensors were tested using bias voltage 140Mv, measured at magnetic 520Oe and applied sweep magnetic field  $\pm 520\text{Oe}$ .

3.4.3 Statistical analysis tool "JMP" software is used for the analysis.



## CHAPTER 4

### RESULTS AND ANALYSIS OF DATA

The experiment of this thesis and the data analysis were performed at Western Digital Bangpa-in manufacturing plant and King Mongkut's Institute of Technology Ladkrabang. All experiments relating to conventional perpendicular magnetic recording (PMR) system was performed on commercially available Quasi Static Tester (QST). The statistical analysis was done using the statistical analysis tool "JMP" software.

This chapter shows and explains result and analysis of experiment data. In this chapter4, there are3 sections, Section 4.1 explains the characteristics of CPP-GMR versus TMR atthe same AR. They were discussed and compared side by side along with the static characteristics trend of CPP-GMR and TMR over AR range. Section 4.2 explains the reliability performance at AR 1.0 of CPP-GMR versus TMR when high temperature and break down voltage were stressed the sensors. Section 4.3 is conclusion of the experiment results for both characteristic and reliability performance.

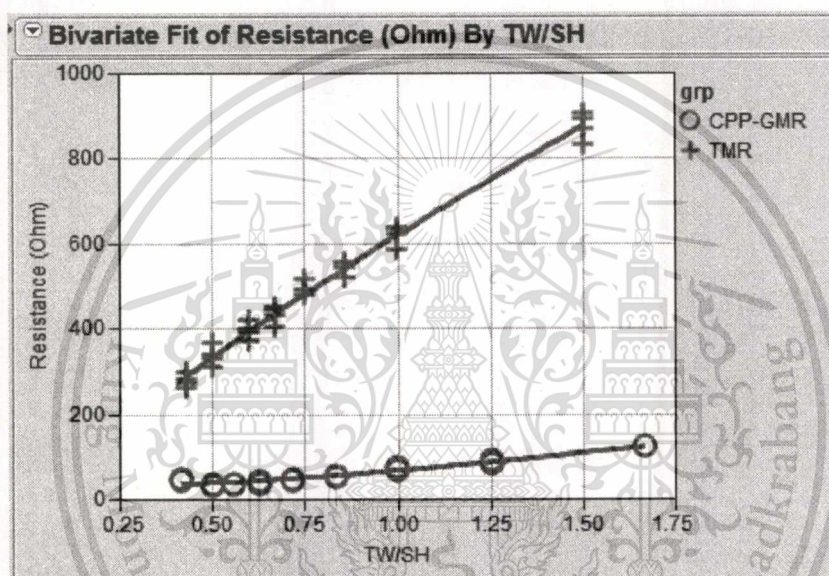
#### 4.1 Characteristics of CPP-GMR versus TMR sensors

CPP-GMR were processed with vary AR from 0.4 to 1.6 then compared to TMR with the same AR. Table 4.1, shows summarization of the characteristics at the same AR 1.0. CPP-GMR shows 7 times lesser resistance than TMR sensor at same AR 1.0., Actual resistance is only 95ohm for CPP-GMR while TMR shows 650ohm. This result shows an opportunity to scale down the reader dimension for both track width and stripe height because of its metal spacer between free layer and pinned layer while current TMR sensor shows very high resistance because of its insulator barrier shown in Figure 4.1. Across AR range, CPP-GMR shows less resistance than TMR. Resistance increases drastically when track width decreases while CPP-GMR shows less sensitivity.

This result confirms that CPP-GMR is a promising candidate for higher areal density  $>2\text{Tbit/in}^2$  due to a space can be scaled down the magnetic read head volume.

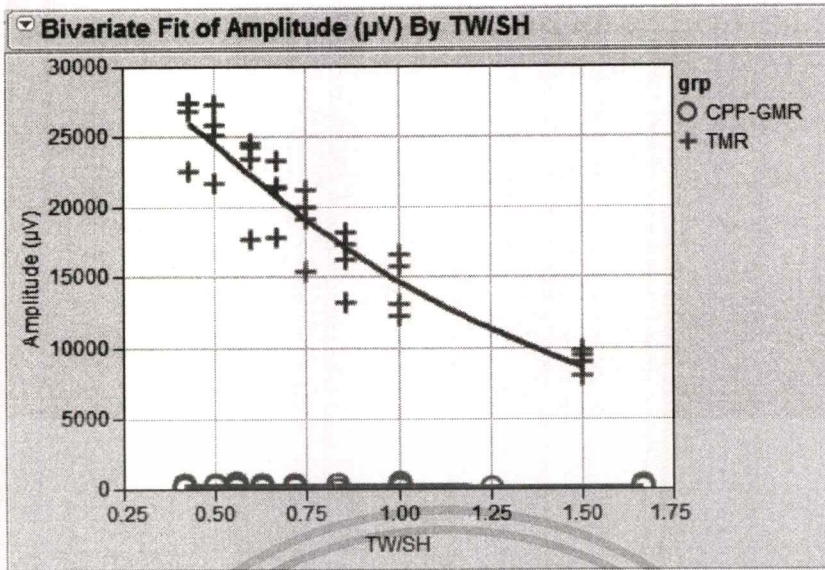
**Table 4.1** Comparison of characteristics between CPP-GMR and TMR sensors at AR 1.0

| Characteristic              | CPP-GMR | TMR   |
|-----------------------------|---------|-------|
| Resistance ( $\Omega$ )     | 95      | 650   |
| Amplitude ( $\mu\text{V}$ ) | 600     | 15000 |
| Static SNR (dB)             | 7.2     | 15.0  |
| Barkhausen Jump (%)         | 19.0    | 2.8   |
| Hysteresis (%)              | 12.4    | 4.2   |

**Figure 4.1** Resistance of CPP-GMR and TMR with different AR

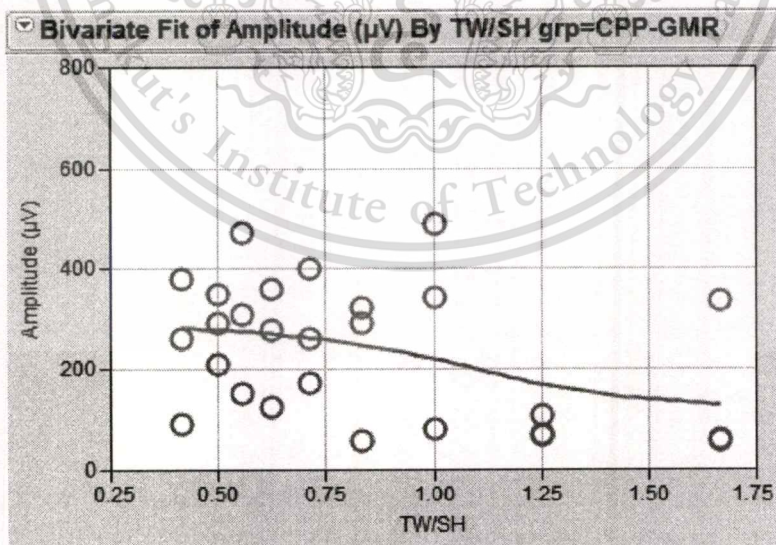
In term of sensitivity or amplitude results, same measurement conditions were performed to characterize both CPP-GMR and TMR sensors. CPP-GMR sensor shows 24 times less amplitude compared to TMR at AR 1.0, actual amplitude is only 600 $\mu\text{V}$  compared to TMR at 15000 $\mu\text{V}$  as shown in Figure 4.2. The amplitude of CPP-GMR is lower than TMR due to lower GMR effect of metal spacers compared to the current TMR effect using insulator barrier.

In order to optimize the CPP-GMR sensor for high areal densities, we need to optimize measurement conditions to find tune the best performance then feedback available experiment results to design team to study and improve performance.



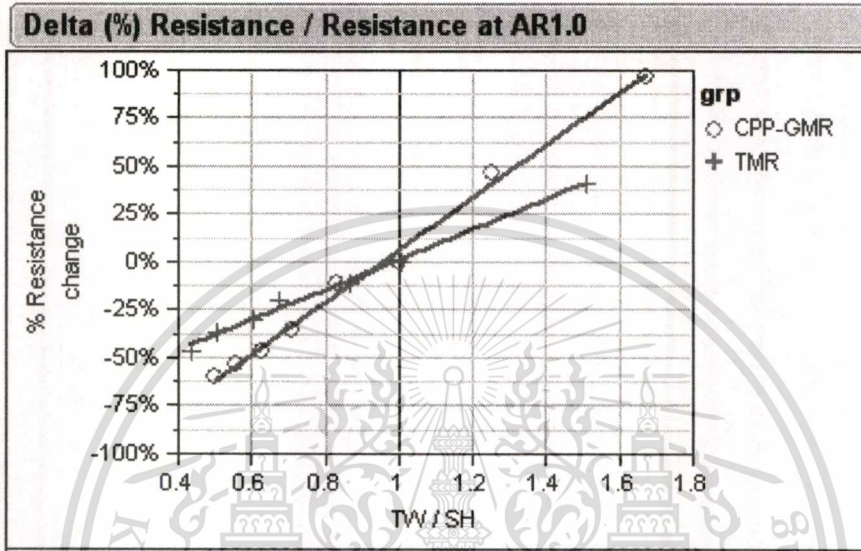
**Figure 4.2** Amplitude of CPP-GMR and TMR with different AR

Figure 4.2 shows that at low AR, both CPP-GMR and TMR sensors show higher amplitude then reduce when AR increases. Amplitude of CPP-GMR gradually decreases when track width is narrow down while TMR rapidly decreases. We zoomed in only CPP-GMR. The results confirm that its amplitude trend is the same as TMR as shown in Figure 4.3.



**Figure 4.3** Zoom-In Amplitude of CPP-GMR with different AR

Percent delta of resistance and amplitude at different AR compared to AR 1.0 is shown in Figure 4.4 and Figure 4.5. These plots show sensitivity of resistance and amplitude of both CPP-GMR in same units. When the magnetic read sensor stripe height is reduced (AR reduced), resistance of CPP-GMR shows more sensitive resistance while less sensitive amplitude when AR changed compared to TMR sensors.



**Figure 4.4** Percent Resistance change at different AR compared to AR1.0

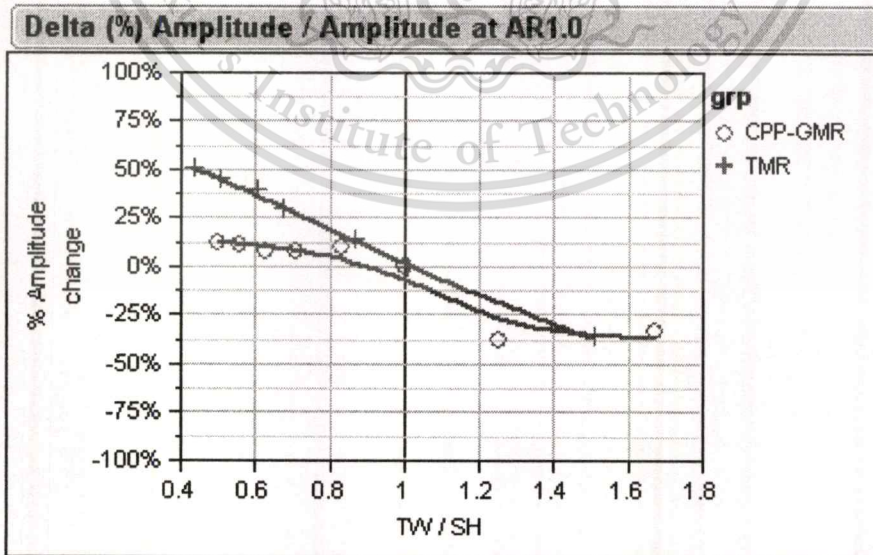


**Figure 4.5** Percent Amplitude change at different AR compared to AR1.0

Figure 4.6 shows static SNR of CPP-GMR sensor. It is lower than TMR  $\sim 3.5$  times at AR 1.0, due to lower amplitude and also lower noise. CPP-GMR and TMR generate different noise phenomena; noise of CPP-GMR contribution is smaller than TMR's. It is because of the absence of shot noise. It is only Johnson noise (thermal noise) which depends on resistance. Both CPP-GMR and TMR show static SNR changed at the same rate. In this study we measured amplitude CPP-GMR at the same condition as TMR, so that CPP-GMR did not show the best performance because it may not be a suitable measurement conditions. At low AR or longer stripe height, it shows better static SNR for both CPP-GMR and TMR, because longer SH contributes higher magnetic read volume which effects to sensitivity, stability and noise.

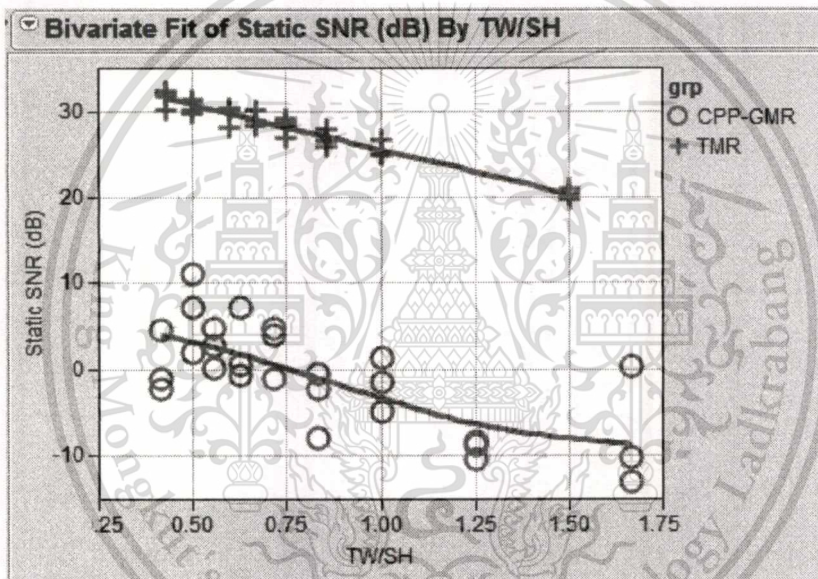


**Figure 4.6** Static SNR of CPP-GMR and TMR with different AR

In term of stability, Barkhausen jump and Hysteresis of CPP-GMR sensors show worse stability than TMR sensors on both Barkhausen jump and Hysteresis. Normally Barkhausen noise and Hysteresis come from domain structures and applied magnetic field, Figure 4.7 and Figure 4.8 show that Barkhausen jump and Hysteresis of CPP-GMR are worse than TMR at all AR range. In this QST measurement, Barkhausen Jump and Hysteresis performed from initial amplitude.

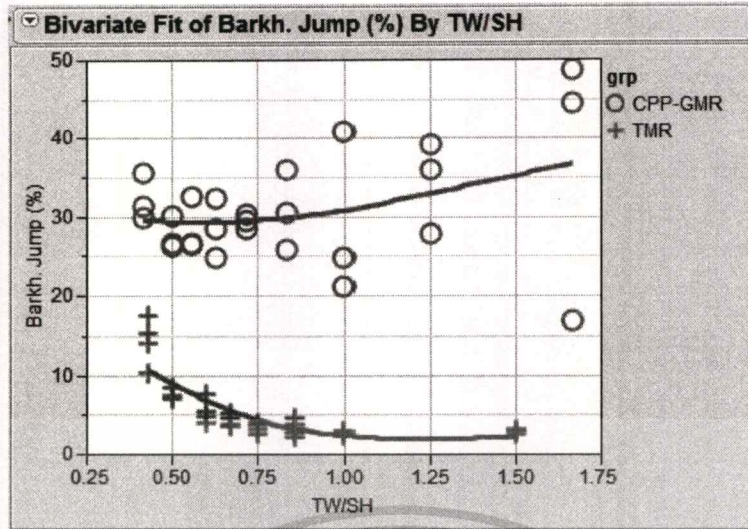


Figure 4.7 Barkhausen Jump (%) of CPP-GMR versus TMR with different AR

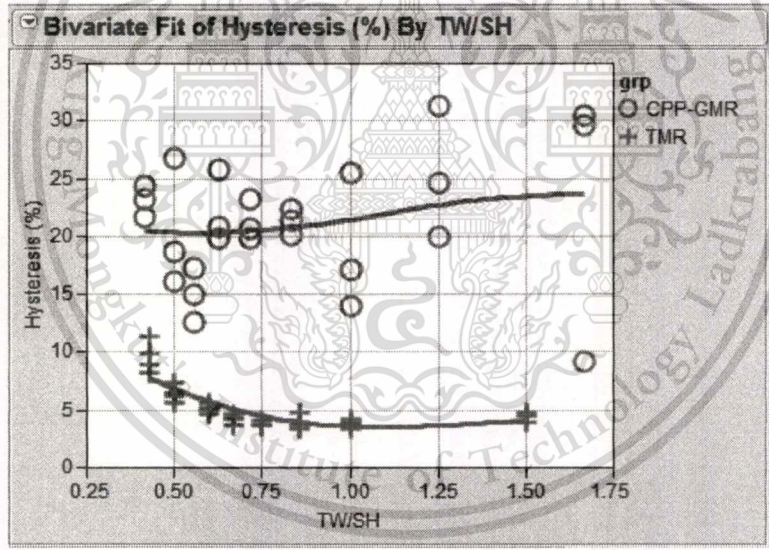


Figure 4.8 Hysteresis (%) of CPP-GMR versus TMR with different AR

### 4.2 Reliability of CPP-GMR versus TMR sensors

In this study, reliability of CPP-GMR and TMR sensors were planned, only AR 1.0 was selected for both CPP-GMR and TMR sensor. There are 2 reliability tests; high temperature stress test and Break down voltage (BDV). They were tested for both sensors. The purpose of high temperature stress test is to study and compare characteristic of CPP-GMR and TMR at high

temperature stress about 120°C. BDV test is to evaluate the quality of metal spacer of CPP-GMR and the barrier of TMR sensor.

High temperature stress test is a reliability test that shows the performance of magnetic read sensors at high temperature. Normally magnetic read sensor should show stable performance or at least not degrade. When the temperature is cool down the performance should be back to the original.

Resistance and amplitude change was measured at normal temperature 20°C, 40°C, 50°C, 70°C, 100°C, 120°C and back to normal temperature then measurement quasi static parameters on all steps. Table 4.2 shows percent of the resistance and amplitude changed of CPP-GMR and TMR sensors. At the highest temperature, 120 degree Celsius, the resistance changes within 10% and then back to normal when the temperature cools down for both CPP-GMR and TMR sensors. In term of amplitude, CPP-GMR shows 30% drop which is worse than TMR which is only 8% drop then both sensors can recovery to the original.

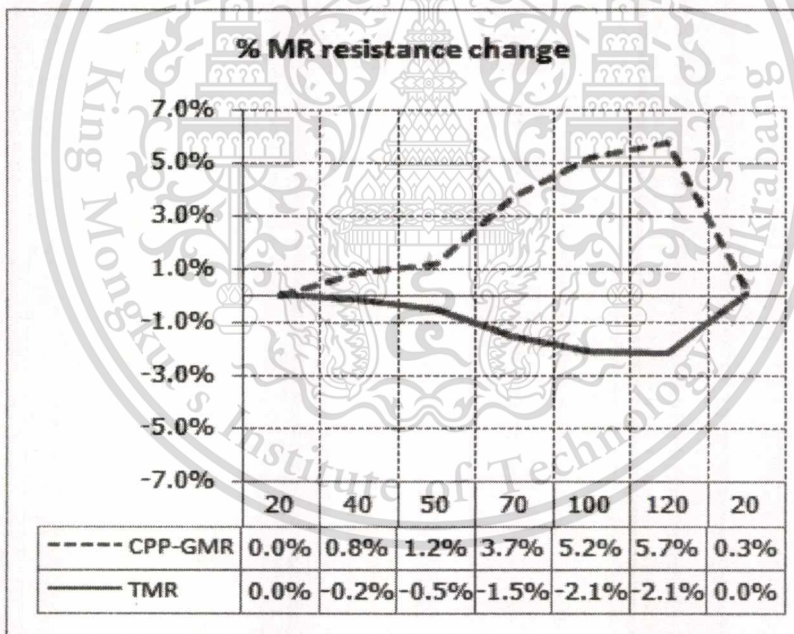


**Figure 4.9** Percent Resistance change at high temperature stress

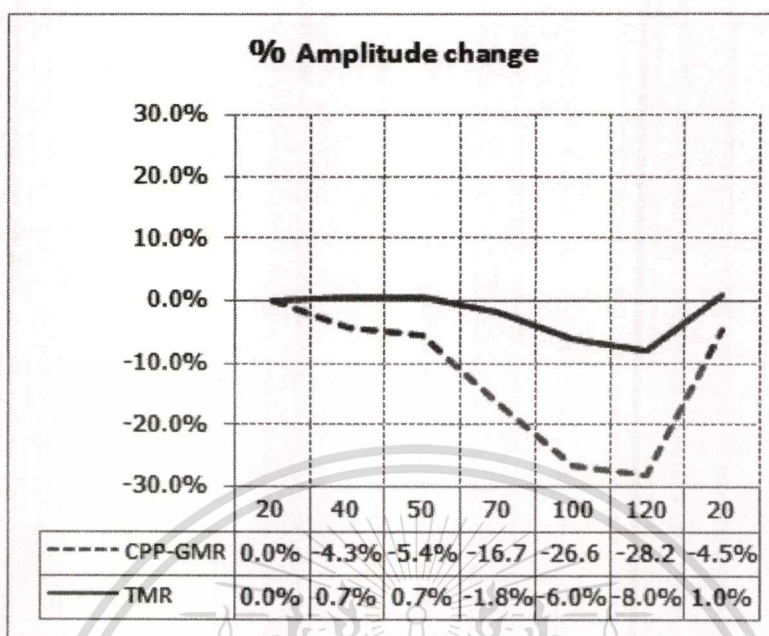


**Figure 4.10** Percent Amplitude change at high temperature stress

**Table 4.2** Resistance and Amplitude of CPP-GMR and TMR at high temperature stress

| Temperature (°C) | CPP-GMR             |                | TMR                 |                |
|------------------|---------------------|----------------|---------------------|----------------|
|                  | MR Resistance (ohm) | Amplitude (uV) | MR Resistance (ohm) | Amplitude (uV) |
| 20               | 49.2                | 403.6          | 596.4               | 12566.3        |
| 40               | 49.6                | 395.4          | 595.2               | 12649.0        |
| 50               | 49.8                | 395.4          | 593.3               | 12657.2        |
| 70               | 51.0                | 325.4          | 587.4               | 12335.0        |
| 100              | 51.8                | 288.3          | 584.1               | 11810.4        |
| 120              | 52.0                | 284.2          | 583.6               | 11558.4        |
| 20               | 49.3                | 378.9          | 596.5               | 12686.1        |

BDV tests start from 0 volt bias then 140mV, increasing to about 600mV with 50mV incremental, resistance and amplitude were measured and focused using QST. We defined break down point to be bias volt that effects to resistance change  $\geq 30\%$ . CPP-GMR and TMR sensors

show different phenomena at high voltage bias. That is the resistance of CPP-GMR increase >30% at BDV average 420mV while TMR's decrease >30% at BDV average 600mV. Although 2 types of magnetic read sensors (CPP-GMR & TMR) show different damage symptom, the results are the same, which is magnetic read sensor cannot work anymore.

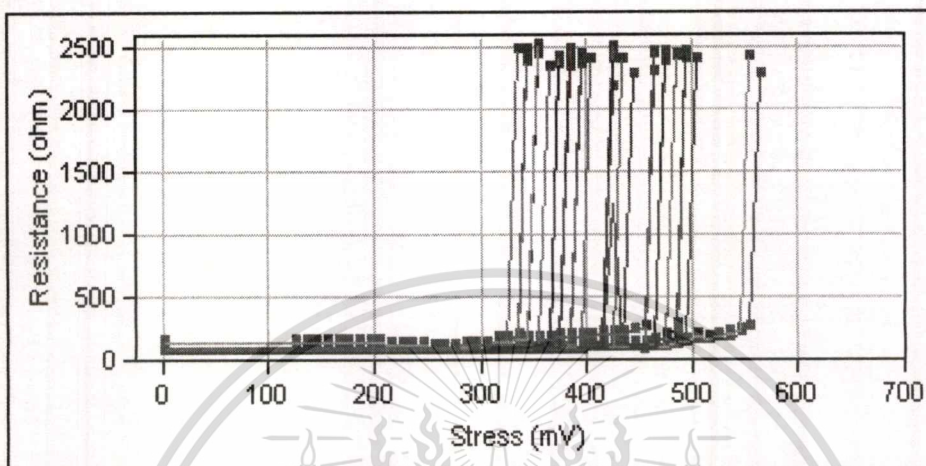


Figure 4.11 Break down voltage test result of CPP-GMR sensors

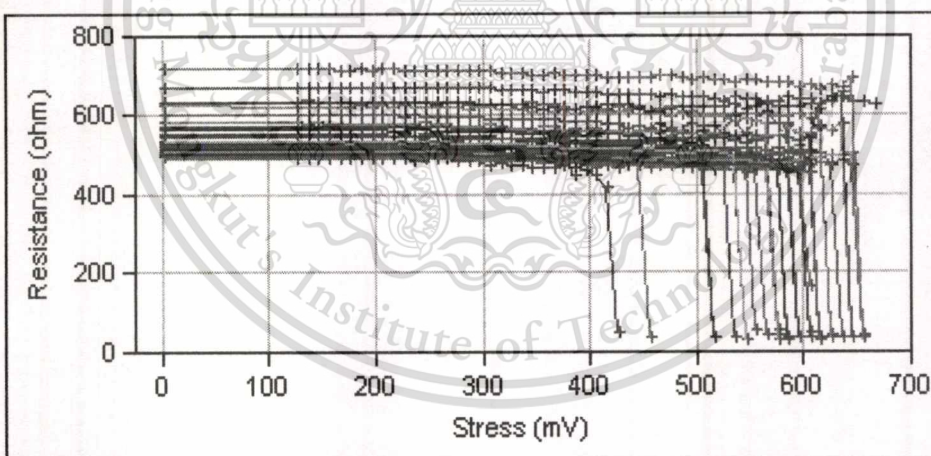


Figure 4.12 Break down voltage test results of TMR sensors

### 4.3 Conclusion

CPP-GMR sensors can be the candidate magnetic read sensor because of its metallic spacer instead of TMR with insulator barrier. TMR read sensor will go against the limit at around 2Tbit/in<sup>2</sup> recording density, because of its high impedance so we cannot scale down the magnetic

read sensor dimensions anymore. It is generally accepted that giant magnetoresistance (GMR) reader using all metallic materials and in current perpendicular to the plane (CPP) geometry has to be employed for areal density  $>2\text{Tbit/in}^2$ . We made the conclusion as follow;

4.3.1 Selected CPP-GMR sensors show an opportunity to scale down the reader dimension for both track width and stripe height because of the metal spacer between free layer and pinned layer while current TMR sensor shows very high resistance because of its insulator barrier. CPP-GMR sensor shows 7 times lesser resistance than TMR sensor at the same AR 1.0 (95ohm versus 650ohm). This result confirms that CPP-GMR is a promising candidate for higher areal density  $>2\text{Tbit/in}^2$  due to a room to scale down the magnetic read head volume.

4.3.2 CPP-GMR sensor shows less sensitivity resistance and amplitude when track width reduced while TMR sensors show high sensitivity.

4.3.3 CPP-GMR sensors show some drawbacks. CPP-GMR sensor shows 24 times less amplitude compared to TMR at AR 1.0. Actual amplitude is only 600uV compared to TMR at 15000uV less sensitivity or amplitude and poor static SNR due to spin valve effects in GMR compared to spintronic effects in TMR sensor. In term of stability, CPP-GMR sensors show worse Barkhausen Jump and Hysteresis than TMR at all AR range.

4.3.4 Reliability of CPP-GMR sensors, there are 2 evaluations in this study, break down voltage and high temperature stress tests. CPP-GMR shows resistance drop of 30% at 120 degree Celsius which is worse than TMR which shows only 8% drop. However at the end, when temperature cools down, both CPP-GMR and TMR sensors can revitalize to its original.

## CHAPTER 5

### CONCLUSIONS AND SUGGESTIONS

In this study, the characteristic and reliability of CPP-GMR and TMR sensors with available perpendicular magnetic recording system (PMR) are proposed and investigated. Problem statements and previous studies of magnetic read sensor issues were reviewed and summarized. Experiments were designed to study characteristic and reliability of CPP-GMR and TMR sensor. Available CPP-GMR and TMR sensors from WD design team which is fabricated slider process at WD Bang pa-in manufacturing plant were employed in this study. We varied magnetic volume by change stripe height and aspect ratio (AR) in order to study the effects of AR on characteristics. Selected CPP-GMR and TMR sensors with AR 1.0 were studied reliability.

#### 5.1 Conclusions and Discussions

The effects of stripe height and aspect ratio (AR) on the characteristics and reliability of the CPP-GMR and TMR sensors are presented. CPP-GMR shows potential and opportunity to scale down the reader dimensions, without large increases in sensor resistance. This is due to the metallic spacer layer between free layer and pinned layer. The current TMR sensor shows very high resistance because of the insulator barrier. In spite of the resistance advantage, the CPP-GMR sensors evaluated in this study do not outperform compared to current TMR sensors, and need further optimizations in amplitude, static SNR and stability Barkhausen Jump and Hysteresis. The reliability of CPP-GMR sensors show resistance and amplitude drop more than TMR at high temperature 120 degree Celsius but can recovery back to original when temperature cool down to room temperature.

The most discouraging challenge for future magnetic read sensor technology will be thermal activated magnetic noise at small dimensions. This challenge is common for both TMR and CPP-GMR sensors, and will limit the smallest practical ferromagnetic sensor volumes or even necessitate a transition to non-magnetic sensor technologies.

## 5.2 Suggestions

In this study we used CPP-GMR sensor which are fabricated in WD US manufacturing plant, they are not feasible to change the magnetic material and other designs except physical dimensions which can be provided in WD Bang pa-in manufacturing plant. Thus we vary only aspect ratio (stripe height and trackwidth ratio). Further evaluation to validate the performance and reliability of magnetic read sensors are suggested and studied.

Suggestion can be made in different topics as follow.

1) Technical knowledge, CPP-GMR shows opportunity to scale down without large resistance increasing. Need to feedback to WD design team to improve CPP-GMR. In this study, available CPP-GMR sensors performed unexpected characteristic and reliability compared to TMR sensors. Further additional magnetic read sensors such as magnetic material, spacer, optimized RA and other layers of sensors need to be considered.

2) Time & Cost saving, we can suggest WD production team to minimize the AR range, reduce sample size and group to achieve suitable AR. We cannot follow standard  $AR = 1$  due to wafer fabrication process cannot control process well.

3) Process improvement, we should check WDB lapping process and consider resistance spec limit to get high quality TMR. (Refer to BDV result)

## REFERENCES

- [1] Han, G. C. Qiu, J. J. Wang, L. Yeo, W. K. and Wang, C. C. "Perspectives of Read Head Technology for 10 Tb/in<sup>2</sup> Recording," **Magnetics, IEEE Transactions on**, vol. 45, pp. 709-714.
- [2] Shiroishi, Y. Fukuda, K. Tagawa, I. Iwasaki, H. Takenoiri, S. Tanaka, H. Mutoh, H. and Yoshikawa, N. "Future Options for HDD Storage," **Magnetics, IEEE Transactions on**, vol. 45, pp. 3816-3822
- [3] Chen, Y. Song, D. Qiu, J. Kolbo, P. Wang, L. He, Q. Covington, M. Stokes, S. Sapozhnikov, V. Dimitrov, D. Gao, K. and Miller, K. "2 Tb/in<sup>2</sup> Reader Design Outlook," **Magnetics, IEEE Transactions on**, vol. 46, pp. 697-701.
- [4] Takagishi, M. Yamada, K. Iwasaki, H. Fuke, H. N. and Hashimoto, S. "Magnetoresistance Ratio and Resistance Area Design of CPP-MR Film for 2- 5 Tb/in<sup>2</sup> Read Sensors," **Magnetics, IEEE Transactions on**, vol. 46, pp. 2086-2089.
- [5] Childress, J. R. and Fontana, R. E. "Magnetic recording read head technology," **C. R. Physics on**, vol. 6, pp 997-1012.
- [6] Gao, K. Z. Heinonen, O and Chen, Y. "Read and write processes , and head technology for perpendicular recording," **Journal of Magnetism and Magnetic Materials**, 321, pp. 495-507.
- [7] Shimazawa, K. Tsuchiya, Y. Mizuno, T. Hara, S. Chou, T. Miyauchi, D. Machita, T. Ayukawa, T. Ichiki, T and Noguchipp, K. "CPP-GMR Film With Zno-Based Novel Spacer for Future High-Density Magnetic Recording," vol. 46, pp. 1487-1490
- [8] Nakamoto, K. Hoshiya, H. Katada, H. Hoshino, K. Yoshida, N. Shiimoto, M. Takei, H. Sato, Y. Hatatani, M. Watanabe. K. Carey, M. Maat, S. and Childress, J. "CPP-GMR Heads With a Current Screen Layer for 300 Gb/in<sup>2</sup> Recording," **Magnetics, IEEE Transactions on**, vol 44, pp. 95-99.
- [9] Nagasaka, K. Jogo, A. Ibusuki, T. Oshima, H. Shimizu, Y. Uzumaki, T. "CPP-GMR Technology for Future High-Density Magnetic Recording," **Fujitsu Science Technology**, vol. 42, pp. 149-157.
- [10] Nagasaka, K. "CPP-GMR technology for magnetic read heads of future high-density recording systems," **Journal of Magnetism and Magnetic Materials**, 321, pp. 508-511.

- [11] Liul, F. Chang<sup>1</sup>, C. H. and Pant, B. B. "Characteristics of Electrostatic Discharge Induced Damage on Magnetic Tunnel Junctions," **INTERMAG 2006**, pp. 279.
- [12] Okabayashi, J. Watanabe, M. Yamaguchi, M. and Yoshino J. "Temperature and bias-voltage dependences of tunneling magnetoresistance in Ga, Mn As based double-barrier magnetic tunnel junctions," **J. Appl. Phys.** 103, 07A908. (2008).
- [13] Cyrille, M. C. Dill, F. Li, J. Fontana, R. Pinarbasi, M. Baer, A. Katine, J. Smith, A. D. Jayasekara, A. D. Mauri, D. Ho M., Mackay, K. and Tsang, C. "Nano Processing Strategies for MR Sensor Read Width and Stripe Height Formation," **Magnetics, IEEE Transactions on**, vol. 44, pp. 2343-2347.
- [14] Mao, S. Chen<sup>1</sup>, Y. Liu, F. Chen, X. Xu, B. Lu, P. Patwari, M. Xi, M. Chang, C. Miller, B. Menard, D. Pant, B. Loven, J. Duxstad, K. Li, S. Zhang, Z. Johnston, A. Lamberton, R. Gubbins, M. McLaughlin, T. Gadbois, J. Ding, J. Cross, B. Xue, S. and Ryan, P. "Commercial TMR Heads for Hard Disk Drives: Characterization and Extendibility At 300 Gbit/in<sup>2</sup>," **Magnetics, IEEE Transactions on**, vol. 42, pp. 97-102.
- [15] Zutic, I. Fabian, J. and Sarma, S. D. "Spintronics: Fundamentals and applications," **Reviews of Modern of Modern Physics**, vol. 76, 2004.



**APPENDIX:**

**CONFERENCE PROCEEDING**

This material is reserved for educational use only, not allowed for commercial use.

Forbidden to modify the content, and cite the document when use.

# Effects of Track Width and Stripe Height Ratio on the Characteristics of CPP-GMR and TMR Heads

<sup>1</sup>S. Kamwan, <sup>2</sup>W. Pijitrojana and <sup>3</sup>C. Sa-ngiamsak  
 Department of Data storage technology and Application  
 King Mongkut's Institute of Technology Ladkrabang  
 Ladkrabang, Bangkok 10520, Thailand

<sup>1</sup>pui082@hotmail.com, <sup>2</sup>pwanchai@engr.tu.ac.th and <sup>3</sup>chiranut@kku.ac.th

**Abstract** - Hard disk drive industry has been facing strong competition from other data storage devices. The primary reader technology based on the Giant magnetoresistance (GMR) and Tunneling magnetoresistance (TMR). TMR head reaches the limit at the 2Tb/in<sup>2</sup> recording density, because of its high impedance affected on the bit rate of the signal. Overcoming the previous limit, CPP-GMR reader using all metallic materials and in current perpendicular to the plane (CPP) geometry has to be employed for areal density >2Tb/in<sup>2</sup>. In this study we focus on physical dimension designs of CPP-GMR head. CPP-GMR still shows the potential gaps of resistance to narrow down the reader size, in terms of static signal to noise ratio (SNR). CPP-GMR shows maximum static SNR at bit aspect ratio (BAR) ~0.6, which suggests that the key physical dimension track width and stripe height ratio should be optimized to achieve static SNR of CPP-GMR sensor. By the way we need to consider more about other design parameters, for examples magnetic materials, Resistance area (RA) and alternative metal spacers.

**Keywords** - CPP-GMR, TMR, Track Width, Stripe Height, Resistance, Amplitude and SNR.

## I. INTRODUCTION

Hard disk drive (HDD) industry has been facing strong competition from other data storage devices such as solid state drive. In order to keep HDD's advantages in cost and capacity, the areal density should be maintained an annual growth rate of 30% to 40% [1]. Fig. 1 shows SCR road map, the hard disk drive (HDD) industry is expected to demonstrate and manufacture the 2 Tbit/in<sup>2</sup> technology and products in the years 2012 and 2015, respectively.

TMR head will hit the wall at around 2 Tb/in<sup>2</sup> recording density, because of its high impedance. It is generally accepted that giant magnetoresistance (GMR) reader using all metallic materials and in current perpendicular to the plane (CPP) geometry has to be employed for areal density >2Tb/in<sup>2</sup> [2]. Then we plan to study the characteristics, reliability and

potential advantages of next-generation magnetic read head especially CPP-GMR sensors.

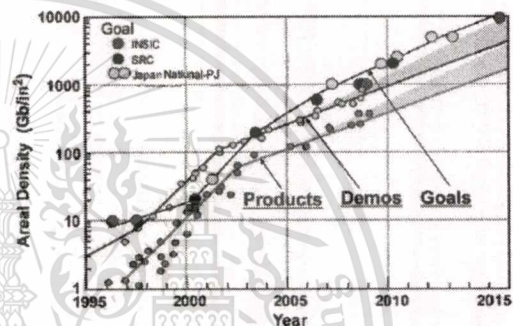


Fig. 1 SCR Road map of May 2009. Original image simplified to highlight reader challenges. Courtesy of Y. Shiroishi. [2]

## II. PRINCIPLES AND THEORIES

### A. Giant Magnetoresistance (GMR)

The invention of the hard-disk drive since the year 1956, the technology of the magnetic head sensor has never been stopped developing to achieve higher areal density. Nowadays magnetic read head sensors are drastically different from early used [3].

Fig. 2 shows the magnetic moment of the giant magnetoresistance (GMR) consisting of ferromagnetic layers and separated by a metal spacer. GMR is the first high volume commercial example of the true magnetic nanotechnology and spintronics. It also introduces a new level of complexity to the practical manufacture of microelectronic devices. The basic magnetoresistive film can be composed of a dozen or more layers of magnetic and nonmagnetic materials whose effective thickness is controlled at the sub-Angstrom level. Each of these layers directly determines or affects the magnetic and magneto transport behavior. The final product needs to be compatible with the unforgiving fabrication and environment of recording

heads designed to fly just a few nanometers above a spinning disk at up to 15000 revolutions per minute [3].

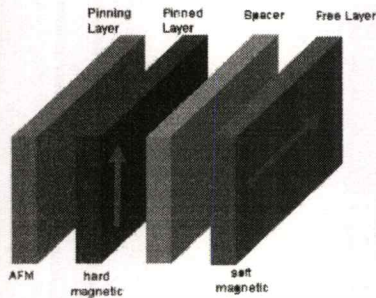


Fig. 2 Schematic of simple spin-valve structure

The giant magnetoresistance (GMR) is possibly the most important of the magnetoresistances, in view of the interest in its physical basis and on its potential for applications. In an experiment with multilayer, the resistance of the ferromagnetic layers depends on the relative directions of the magnetization and electron spin. This discovery is regarded as an important breakthrough that opens the way to the development of spin electronics, or spintronics. The simplest quantitative description of the GMR effect is afforded by the model of resistance; the electrical resistance of a multilayer structure traversed by a current of electrons with spin up and spin down is equivalent to a resistance of a circuit with two parallel branches of resistors. When the magnetizations of the ferromagnetic layers are parallel, the equivalent circuit has resistors with small resistance in series in one branch, and large resistance in the other. When the magnetizations of the layers alternate their directions, the parallel circuits contain both large and small resistances. The resistances for the two arrangements of the multilayer are parallel magnetic layers (RP) and anti-parallel layers (RAP). [4]

#### B. Current perpendicular to plane

The GMR effect can be studied in two geometries: 1) with a current applied in the plane of the multilayer - current in plane (CIP) or 2) with a current applied perpendicularly to the plane (CPP) as shown in Fig. 3.

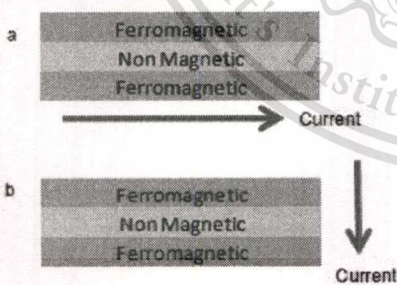


Fig. 3 Different geometrics of giant magnetoresistance  
(a) CIP-GMR (b) CPP-GMR

As sensor dimensions continue to decrease, several factors are contributing to performance limitations for CIP-GMR sensors, which necessitate further evolution in sensor design. First, as density increases both read Track Width (TW) and Shield to Shield spacing (SS) must be decreased. Since the sensor current travels parallel to TW, this implies that the length of the sensors must continuously be decreased, and therefore the sensor height or stripe height (SH) above the disk must also be decreased to keep the sensor resistance and the signal constant. If this simple scaling cannot be accomplished, or if edge effects reduce the effective signal, then the intrinsic GMR ratio must be increased proportionally to keep the output signal constant.

However, the GMR of practical spin-valve devices appears to be limited to 20% at the most, close to current technology. Furthermore, as SS decreased, it becomes more difficult to fit low-resistance electrical leads between the shields, which increases the parasitic resistance and reduces the effective signal.

Fig. 4 reveals the reader volume and dimensions of CIP-GMR vs. CPP-GMR; (a) CPP geometry can eliminate the SS dimension by using shield as electrodes and (b) the current direction of CIP vs. CPP GMR heads.

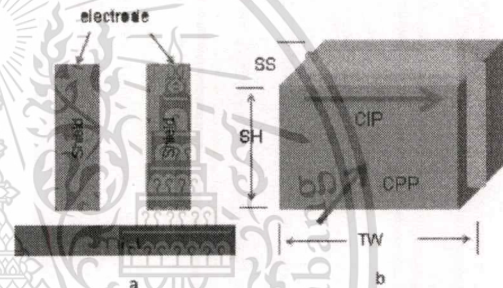


Fig. 4 (a) CPP read head in which the shields can also be used as the electrodes which help to eliminate the SS, (b) Sensor element used in both the CPP and CIP modes.

### III. KEY DESIGNS FOR FUTURE MAGNETIC READING HEAD

The common driving force for any type of data storage technology is the areal density [1]. CPP-GMR is one of potential candidates for future reader sensors applied with low RA, low noise and fast data transfer rate and high area density [4, 5]. In this study we focus on physical dimension designs 1) read Track Width (TW). We need to scale down TW to increase track density as much as possible. 2) Stripe Height (SH), which is important for reader volume. SH must be also decreased to keep the sensor resistance and the signal constant. 3) Shield to Shield spacing (SS), or the distance between top shield and bottom shield. This dimension needs to be scaled down to increase bit density.

The definition of scaled parameters is given in Fig. 5. Those physical parameters need to be optimized to achieve the best characterization, reliability and areal density.

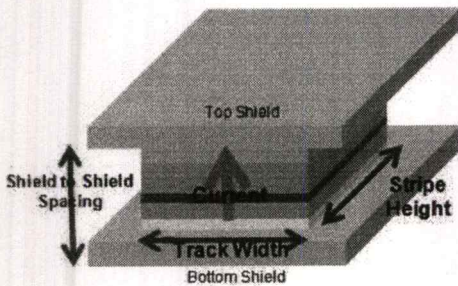


Fig. 5 Physical dimension for magnetic read head

#### IV. CHARACTERIZATION FOR MAGNETIC READ SENSOR

The characterization and reliability of CPP-GMR have been done by using the quasi static tester (QST). QST is a test equipment that can characterize the performance of magnetic recording heads without performing flying head over the recording media. Principle of QST test is to apply bias current to recording heads, and then the recording head resistance is obtained, which is calculated from applied current and voltage across the device. The external magnetic field is applied by sweeping from negative to positive fields, and then the transfer curve of magnetic recording heads is also obtained as Fig. 6.

To use QST, we focus on many key parameters. There are basic magnetic properties such as (1) Magnetic read head resistance, which is measured by applying current,  $I_{bias}$ , pass through the read head sensor and the voltage is measured across the read head sensor, and then the resistance is calculated. (2) Amplitude, basically we measure 2 types of QST amplitude test, which are amplitude at test and peak to peak amplitude. Amplitude at test is peak amplitude at the point that user defines field location, based on average value of the forward and reverse curves. Peak to peak amplitude is calculated from maximum and minimum amplitudes.

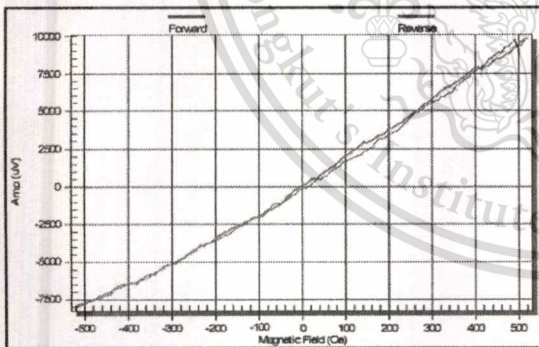


Fig. 6 Transfer curve (TC) of Magnetic recording head

In this study we also focus on signal to noise ratio (SNR), here the SNR is static SNR which is measured by QST. SNR is

a key to be focused on magnetic read head sensors which is calculated from amplitude divided by noise. Higher or optimum SNR is required for future magnetic read head CPP-GMR design.

#### V. EXPERIMENTAL RESULTS AND SUMMARY

We perform the experiments to study characteristic and reliability of CPP-GMR purposely to answer how to design future magnetic read head, especially CPP-GMR, to achieve higher areal density by using quasi static tester.

The results of the experiments are useful for understanding, development and future magnetic recording head designs, especially the near future candidate CPP-GMR sensor.

The characterization of initial CPP-GMR with different bit aspect ratio (BAR) which is calculated from

$$BAR = TW / SH \quad (1)$$

where BAR is bit aspect ratio, TW is read track width and SH is stripe height of read head. Equation (1) shows the ratio of TW and SH or refers reader volume. If BAR is equal to 1.0, it means that the read track width and stripe height dimension are equal. In the other hands, if BAR is less than 1, it means that read track width dimension is narrower than stripe height.

We perform CPP-GMR designs with BAR scanning from 0.4 to 1.6 compared to TMR with the same BAR. Fig. 7 shows the resistance of both CPP-GMR and TMR. It shows the same trend; low resistance at low BAR, and then it increases at higher BAR or short SH. If we want to increase areal density, we need to scale down the TW and also SH to increase track density. CPP-GMR shows 7 times smaller resistance compared to TMR at BAR equal 1.0. This shows an opportunity to scale down the reader dimension for TW and SH because of the metal spacer between free layer and pinned layer while current TMR sensor shows very high resistance because of insulator barrier. This result confirms that CPP-GMR is a promising candidate for higher areal density  $>2Tbit/in^2$  due to a room to scale down the magnetic read head volume.

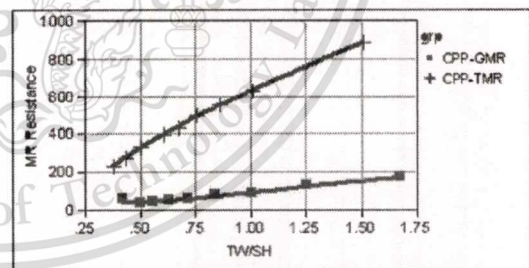


Fig. 7 Resistance of CPP-GMR and CPP-TMR with different BAR

Fig. 8 shows amplitude of sensitivity comparison, CPP-GMR shows 24 times less amplitude compared to TMR at same BAR equal 1.0. The amplitude of CPP-GMR is lower than TMR due to lower  $\Delta R/R$  of metal spacer spin valves effect compared to insulator barrier tunneling effect in TMR. If

we want higher areal density by the best choice, CPP-GMR is needed to be optimized between the acceptable amplitude or sensitivity and opportunity of resistance to scale down the reader volume. The amplitude of CPP-GMR is tracks to BAR same as TMR as shown in Fig. 9. At lower BAR, 0.3 to 0.6, it shows high amplitude, and then it decreases when BAR increases. For TMR, it is different and it shows optimum amplitude at BAR  $\sim 0.5$ . If TW is scaled down, SH is also optimized to achieve more amplitude.

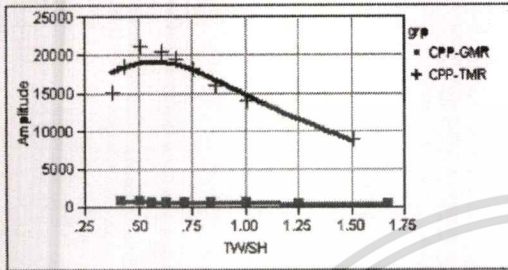


Fig. 8 Amplitude of CPP-GMR and CPP-TMR with different BAR

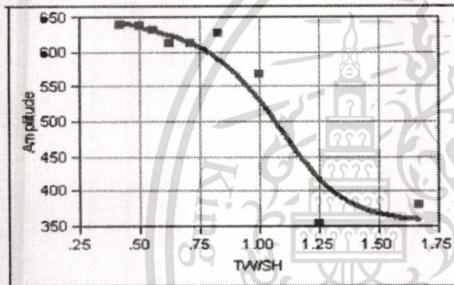


Fig. 9 Zoom-In Resistance & Amplitude of CPP-GMR

Fig. 10 shows static SNR of CPP-GMR sensor. It is lower than TMR  $\sim 3.5$  times at same BAR equal 1.0, due to lower amplitude and also lower noise. CPP-GMR and TMR generate different noise phenomena. Noise of CPP-GMR contributions is smaller than of TMR. It is because of the absence of shot noise. It is only Johnson noise (thermal noise) which depends on resistance.

At low BAR or longer SH, it shows better static SNR for both CPP-GMR and TMR, due to longer SH contributes higher magnetic read volume which effects to sensitivity, stability and noise.

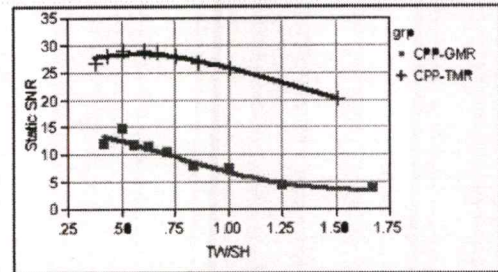


Fig. 10 Static SNR of CPP-GMR and CPP-TMR with different BAR

## VI. CONCLUSION

The effects of track width and stripe height ratio on the characteristics of the CPP-GMR and TMR heads are presented. CPP-GMR shows potential and opportunity to scale down the reader volume to achieve higher areal density. This is because of the metallic spacer layer between free layer and pinned layer. The current TMR sensor shows very high resistance because of insulator barrier. In the future we need to optimize other designs and need to consider more for the acceptable amplitude, SNR and other parameters for characterization.

The most daunting challenge for future read sensor technology will be thermal activated magnetic noise at small dimensions of TW, SS and SH, which will limit the smallest practical ferromagnetic sensor volume, or necessitate a transition to non-magnetic sensor technologies.

## ACKNOWLEDGMENT

The author would like to thank Western Digital Company Thailand for financial support and Device optimization engineering team for experimental support.

## REFERENCES

- [1] J. R. Childress, R. E. Fontana, "Magnetic recording read head technology," *C. R. Physics on*, vol. 6, pp.997-1012.
- [2] Y. Chen, D. Song, J. Qiu, P. Kolbo, L. Wang, Q. He, M. Covington, S. Stokes, V. Sapozhnikov, D. Dimitrov, K. Gao, and B. Miller, "2 Tb/in<sup>2</sup> Reader Design Outlook," *Magnetics, IEEE Transactions on*, vol. 46, pp. 697-701.
- [3] M. Takagishi, K. Yamada, H. Iwasaki, H. N. Fuke, and S. Hashimoto, "Magnetoresistance Ratio and Resistance Area Design of CPP-MR Film for 2-5 Tb/in<sup>2</sup> Read Sensors," *Magnetics, IEEE Transactions on*, vol. 46, pp. 2086-2089.
- [4] K. Nakamoto, H. Hoshiya, H. Katada, K. Hoshino, N. Yoshida, M. Shiimoto, H. Takei, Y. Sato, M. Hatatani, K. Watanabe, M. Carey, S. Maat and J. Childress, "CPP-GMR Heads With a Current Screen Layer for 300 Gb/in<sup>2</sup> Recording," *Magnetics, IEEE Transactions on*, vol 44, pp95-99.
- [5] N. Keiichi, J. Arata, I. Takahiro, O. Hirofuka, S. Yutaka, U. Takuya, "CPP-GMR Technology for Future High-Density Magnetic Recording," *Fujitsu Science Technology*, vol. 42, pp. 149-157.

## BIOGRAPHY

**Name:** Miss Saowarat Kamwan

**Date of Birth:** 9 August 1980

**Address:** Pathumthani , Thailand

### Education:

2009 – 2011 Master degree, Faculty of Education, Major in Science Teaching from Ramkhamhang University.

1998 - 2003 Bachelor degree, Faculty of Science, Major in Physics and Minor in Mathematics from Chiangmai University.

1992 – 1997 High school from Sapphawitthayakhom School, Tak province.

### Work Experiences:

- 2010 to present, Integration Development Engineer at Western Digital Bang pa-in. Pranakorn Sri Ayutthaya province, Thailand.
- May 2007 – 2010, Device Optimization Engineer at Western Digital Bang pa-in. Pranakorn Sri Ayutthaya province, Thailand.
- 2003 - April 2007, Production Engineer at NEC/token electronics. Pathumthani, Thailand.